

Dynamics of cardiac neutrophil diversity in murine myocardial
infarction

Dynamik der Diversität kardialer neutrophiler Granulozyten im
Mausmodell Herzinfarkt



Doctoral thesis for a medical doctoral degree
at the Graduate School of Life Sciences,
Julius-Maximilians-Universität Würzburg,
Section Biomedizin

submitted by

Laura Krampert
from Darmstadt

Würzburg 2023

Submitted on:

Office stamp

Members of the Thesis Committee:

Chairperson: Prof. Dr. med. Stefan Störk

Primary Supervisor: Ph.D. Clément Cochain

Supervisor (Second): Prof. Dr. Alma Zerneck-Madsen

Supervisor (Third): Prof. Dr. med. Ulrich Hofmann

Supervisor (Fourth): Prof. Dr. med. Süleyman Ergün

Date of Public Defence:

Date of Receipt of Certificates:

Affidavit

I hereby confirm that my thesis entitled “Dynamics of cardiac neutrophil diversity in murine myocardial infarction” is the result of my own work. I did not receive any help or support from commercial consultants. All sources and / or materials applied are listed and specified in the thesis.

Furthermore, I confirm that this thesis has not yet been submitted as part of another examination process neither in identical nor in similar form.

Place, Date

Signature

Eidesstattliche Erklärung

Hiermit erkläre ich an Eides statt, die Dissertation „Dynamik der Diversität kardialer Neutrophiler Granulozyten im Mausmodell Herzinfarkt“ eigenständig, d.h. insbesondere selbstständig und ohne Hilfe eines kommerziellen Promotionsberaters, angefertigt und keine anderen als die von mir angegebenen Quellen und Hilfsmittel verwendet zu haben.

Ich erkläre außerdem, dass die Dissertation weder in gleicher noch in ähnlicher Form bereits in einem anderen Prüfungsverfahren vorgelegen hat.

Ort, Datum

Unterschrift

Table of content

SUMMARY	8
ZUSAMMENFASSUNG	10
1. INTRODUCTION.....	12
1.1. INFLAMMATION FOLLOWING MYOCARDIAL INFARCTION	12
1.2. DETRIMENTAL EFFECTS OF NEUTROPHILS IN MYOCARDIAL INFARCTION	13
1.3. PROTECTIVE FUNCTIONS OF NEUTROPHILS IN MYOCARDIAL INFARCTION	14
1.4. NEUTROPHIL HETEROGENEITY.....	16
1.5. PRELIMINARY DATA.....	19
1.6. AIM OF MY WORK	21
2. MATERIALS	22
2.1. ANIMAL MODEL.....	22
2.2. ANTIBODIES.....	22
2.3. GENERAL CHEMICALS AND REAGENTS	23
2.4. DEVICES.....	24
2.5. SOFTWARE	24
3. METHODS	25
3.1. MYOCARDIAL INFARCTION MODEL IN MICE	25
3.2. EXCLUSION CRITERIA.....	25
3.3. CELL ISOLATION	26
3.3.1. <i>Enzymatic processing of the heart for cell isolation</i>	26
3.3.2. <i>Mechanical processing of the heart for cell isolation</i>	26
3.3.3. <i>Processing of the bone marrow for cell isolation</i>	27
3.3.4. <i>Processing of the blood for cell isolation</i>	27
3.3.5. <i>Processing of the spleen for cell isolation</i>	27
3.4. ORGAN FREEZING AND IMMUNOHISTOLOGICAL STAINING.....	28
3.4.1. <i>Organ freezing and preparation of cryosections</i>	28
3.4.2. <i>Immunohistological staining and imaging</i>	28
3.5. CELL COUNTING	29
3.6. FLOW CYTOMETRY	29
3.6.1. <i>Fluorescence activated cell sorting FACS</i>	29
3.6.2. <i>Staining of surface markers</i>	30
3.7. NEUTROPHIL ACTIVITY ASSAYS	32
3.7.1. <i>ROS production activity assay</i>	32
3.7.2. <i>Phagocytosis activity assay</i>	33
3.8. IN VIVO DEPLETION OF NEUTROPHILS TO INVESTIGATE TIME-DEPENDENT ROLES AND FUNCTIONAL IMPACTS OF NEUTROPHIL SUBPOPULATIONS	34
3.9. CALCULATIONS AND STATISTICAL ANALYSES	35
4. RESULTS	36
4.1. APPEARANCE OF SIGLECF+ NEUTROPHILS IN THE INFARCTED HEART AT DAY 3 POST-MI.....	36
4.2. ABSENCE OF SIGLECFHIGH NEUTROPHILS IN BONE MARROW, BLOOD AND SPLEEN	38
4.2.1. <i>Absence of SiglecFhigh neutrophils in the bone marrow</i>	39
4.2.2. <i>Absence of SiglecFhigh neutrophils in the blood</i>	39
4.2.3. <i>Absence of SiglecFhigh neutrophils in the spleen</i>	40
4.3. VALIDATION EXPERIMENT	41
4.3.1. <i>Heart</i>	41
4.3.2. <i>Blood</i>	42
4.4. IMMUNOFLUORESCENCE LOCALIZATION OF SIGLECF+ CELLS IN THE INFARCTED AREA	43
4.5. CARDIAC NEUTROPHIL SUBSETS SHOW DIFFERENCES IN MAJOR FUNCTIONAL CAPACITIES	44

4.5.1.	<i>Phagocytosis</i>	44
4.5.2.	<i>ROS production</i>	46
4.6.	INVESTIGATION OF THE TIME-DEPENDENT ROLE AND FUNCTIONAL IMPACT OF NEUTROPHIL SUBPOPULATIONS – DEPLETION EXPERIMENTS.....	48
4.6.1.	<i>Neutrophils can be identified independently of Ly6G by detecting them via CXCR2</i>	48
4.6.2.	<i>Anti-Ly6G treatment fails to achieve successful neutrophil depletion at day 3 post-MI</i>	50
4.6.3.	<i>Confirmation of unefficient anti-Ly6G depletion of neutrophils 1 and 3 days after myocardial infarction</i>	57
5.	DISCUSSION	64
5.1.	TIME-DEPENDENT PRESENCE OF DIFFERENT NEUTROPHIL STATES.....	64
5.2.	UNIQUE SIGLEC ^{FHIGH} STATE IN THE ISCHEMIC HEART - A TISSUE RESTRICTED SPECIFICATION	64
5.3.	DIFFERENCES IN FUNCTIONAL CAPACITIES.....	65
5.4.	DEPLETION OF NEUTROPHILS VIA ANTI-LY6G-ANTIBODIES FAILED TO FULLY DEplete CARDIAC NEUTROPHILS BUT INDUCED A SHIFT TO MORE SIGLEC ^{FHIGH} NEUTROPHILS	66
5.5.	SIGLEC ^{FHIGH} NEUTROPHILS CAN ALSO BE FOUND IN DIFFERENT PATHOGENIC SITES.....	68
6.	ANNEX	75
6.1.	TABLE OF FIGURES.....	75
6.2.	LIST OF ABBREVIATIONS.....	77
6.3.	PUBLICATION LIST	78
6.4.	ACKNOWLEDGEMENTS.....	78
6.5.	CURRICULUM VITAE.....	79

Summary

After myocardial infarction, an inflammatory response is induced characterized by a sterile inflammation, followed by a reparative phase in order to induce cardiac healing. Neutrophils are the first immune cells that enter the ischemic tissue. Neutrophils have various functions in the ischemic heart, such as phagocytosis, production of reactive oxygen species or release of granule components. These functions can not only directly damage cardiac tissue, but are also necessary for initiating reparative effects in post-ischemic healing, indicating a dual role of neutrophils in cardiac healing after infarction.

In recent years, evidence has been growing that neutrophils show phenotypic and functional differences in distinct homeostatic and pathogenic settings.

Preliminary data of my working group using single-cell RNA-sequencing revealed the time-dependent heterogeneity of neutrophils, with different populations showing distinct gene expression profiles in ischemic hearts of mice, including the time-dependent appearance of a SiglecF^{high} neutrophil population. To better understand the dynamics of neutrophil heterogeneity in the ischemic heart, my work aimed to validate previous findings at the protein level, as well as to investigate whether the distinct neutrophil populations show functional differences. Furthermore, *in vivo* depletion experiments were performed in order to modulate circulating neutrophil levels.

Hearts, blood, bone marrow and spleens were processed and analyzed from mice after 1 day and 3 days after the onset of cardiac ischemia and analyzed using flow cytometry.

Results showed that the majority of cardiac neutrophils isolated at day 3 after myocardial infarction were SiglecF^{high}, whereas nearly no SiglecF^{high} neutrophils could be isolated from ischemic hearts at day 1 after myocardial infarction.

No SiglecF^{high} neutrophils could be found in the blood, spleen and bone marrow either after 1 day or 3 days after myocardial infarction, indicating that the SiglecF^{high} state of neutrophils is unique to the ischemic cardiac tissue.

When I compared SiglecF^{high} and SiglecF^{low} neutrophils regarding their phagocytosis activity and ROS production, SiglecF^{high} neutrophils showed a higher phagocytosis ability than their SiglecF^{low} counterparts, as well as higher ROS production capacity.

In vivo depletion experiments could not achieve successful and efficient depletion of cardiac neutrophils either 1 day or 3 days after myocardial infarction, but led to a shift of a higher percentage of SiglecF^{high} expressing neutrophils in the depletion group. Bone marrow neutrophil levels only showed partial depletion at day 3 after MI. Regarding blood neutrophils, depletion efficiently reduced circulating neutrophils at both time points, 1 and 3 days after MI. To summarize, this work showed the time-dependent presence of different neutrophil states in the ischemic heart. The main population of neutrophils isolated 3 days after MI showed a high expression of SiglecF, a unique state that could not be detected at different time points or other organs. These SiglecF^{high} neutrophils showed functional differences regarding their phagocytosis ability and ROS production. Further investigation is needed to reveal what role these SiglecF^{high} neutrophils could play within the ischemic heart.

To better target neutrophil depletion in vivo, more efficient or different anti-neutrophil strategies are needed.

Zusammenfassung

Nach Myokardinfarkt kommt es zu einer Entzündungsantwort, die durch eine sterile Entzündung und nachfolgende reparative Phase gekennzeichnet ist, um eine kardiale Heilung zu initiieren. Neutrophile Granulozyten sind die ersten Immunzellen, die das ischämische Gewebe infiltrieren. Neutrophile Granulozyten haben verschiedene Funktionen im ischämischen Herz, wie beispielsweise Phagozytose, Produktion reaktiver Oxigenspezies oder Entleerung von Granulae. Diese Funktionen können nicht nur das kardiale Gewebe direkt schädigen, sondern sind auch notwendig, um die reparative Phase zu initiieren, was auf eine duale Rolle der neutrophilen Granulozyten hinsichtlich kardialer Heilung hinweist.

Evidenz der letzten Jahre zeigt, dass neutrophile Granulozyten phänotypische und funktionelle Unterschiede zeigen, sowohl in Homöostase als auch in verschiedenen pathologischen Umgebungen.

Vorliegende Ergebnisse meiner Arbeitsgruppe von Einzelzellsequenzierungen zeigten die zeitabhängige Heterogenität neutrophiler Granulozyten, die in verschiedenen Populationen und mit unterschiedlichen Expressions-Mustern in ischämischen Mäuseherzen auftauchen. Unter anderem zeigte sich das zeitabhängige Auftauchen einer SiglecF^{high} Neutrophilen-Population. Um die Dynamik der Neutrophilen-Heterogenität im ischämischen Herz besser zu verstehen, war es das Ziel meiner Arbeit, vorliegende Ergebnisse auf Proteinbasis zu bestätigen, und die verschiedenen Neutrophilen-Populationen hinsichtlich möglicher funktioneller Unterschiede zu untersuchen. Zusätzlich wurden in-vivo Depletionsversuche durchgeführt, um das Vorkommen zirkulierender neutrophiler Granulozyten zu modulieren und mögliche Änderungen hinsichtlich des Vorkommens neutrophiler Granulozyten im Herzen zu untersuchen.

Herz, Blut, Knochenmark und Milz von Mäusen, die einen 1 oder 3 Tage alten Myokardinfarkt hatten, wurden prozessiert und mittels Durchflusszytometrie analysiert. Es zeigte sich, dass der überwiegende Anteil kardialer neutrophiler Granulozyten die an Tag 3 nach Myokardinfarkt isoliert wurden SiglecF^{high} waren, wohingegen quasi keine SiglecF^{high} neutrophile Granulozyten an Tag 1 nach Myokardinfarkt gefunden werden konnten.

Es konnten keine SiglecFhigh neutrophile Granulozyten in Blut, Knochenmark oder Milz gefunden werden, weder 1 noch 3 Tage nach Myokardinfarkt, was darauf hinweist, dass der SiglecFhigh Status neutrophiler Granulozyten spezifisch für ischämisches Herzgewebe ist.

Im Vergleich von SiglecFhigh und SiglecFlow neutrophilen Granulozyten hinsichtlich der Phagozytose und Produktion reaktiver Oxigenspezies, zeigten SiglecFhigh neutrophile Granulozyten sowohl eine höhere Phagozytose als auch eine höhere Produktion reaktiver Oxigenspezies.

In vivo Depletionsversuche konnten keine komplette und effiziente Depletion kardialer neutrophiler Granulozyten sowohl an Tag 1 als auch an Tag 3 nach Myokardinfarkt erzielen, führten jedoch zu einem höheren Prozentsatz an SiglecFhigh neutrophilen Granulozyten in der Depletionsgruppe. Neutrophile Granulozyten im Knochenmark konnten nur an Tag 3 teilweise depletiert werden. Mit Blick auf neutrophile Granulozyten im Blut führte die Depletion zu einer effizienten Reduktion zirkulierender neutrophiler Granulozyten sowohl an Tag 1 als auch an Tag 3 nach Myokardinfarkt.

Zusammenfassend zeigt diese Arbeit die zeitabhängige Präsenz verschiedener neutrophiler Granulozyten im ischämischen Herzen. Der größte Anteil neutrophiler Granulozyten, die an Tag 3 isoliert wurden, zeigten eine hohe Expression von SiglecF, einem spezifischen und einzigartigem Phänotypus, der weder zu anderen Zeitpunkten noch in anderen Organen gefunden wurde. Diese SiglecFhigh neutrophilen Granulozyten zeigten funktionelle Unterschiede hinsichtlich ihrer Phagozytose und Produktion reaktiver Oxigenspezies.

Weitere Untersuchungen sind notwendig um aufzuzeigen, welche Rolle diese SiglecFhigh neutrophilen Granulozyten im ischämischen Herzen spielen könnten.

Um eine effizientere Depletion neutrophiler Granulozyten in vivo zu erzielen, sind andere oder effizientere Anti-Neutrophilen Strategien notwendig.

1. Introduction

1.1. Inflammation following myocardial infarction

Myocardial infarction (MI) is the leading cause of morbidity and mortality in western countries. The lack of oxygen leads to ischemia, which causes a massive loss of cardiomyocytes and cardiac tissue and induces a subsequent inflammatory response in order to induce cardiac repair processes (1) (2). This inflammatory response can be divided into different phases. The early inflammatory phase, which occurs during the first days after the onset of ischemia, is characterized by intense sterile inflammation and infiltration of various immune cells in order to digest and clear damaged cells and extracellular matrix tissue. A reparative phase follows, characterized by the resolution of inflammation as well as proliferation of myofibroblasts, scar formation and neovascularization (2) (3). A timed balance between these phases and resolution of inflammation is necessary to provide optimal cardiac repair.

The cell damage that is caused by ischemia leads to the release of molecules such as damage-associated molecular patterns (DAMPs), initiating neutrophil recruitment (4) (5). Attracted by cell debris and inflammatory mediators, neutrophils are the first inflammatory cells recruited to the injured site within hours post-MI (6) (3). Given their main functions, they aim to phagocytose and clear dead cell debris at the site of injury. Neutrophils also release high levels of reactive oxygen species (ROS), proteolytic enzymes and inflammatory mediators necessary for degrading necrotic tissue, which at the same time can directly cause tissue injury (5) (6) (7). Historically considered generally detrimental in the setting of MI, today's view is changing as neutrophils can not only promote or aggravate myocardial injury, but are also necessary for the resolution of inflammation and cardiac repair by exerting anti-inflammatory, pro-angiogenic and pro-reparative effects (8) (9).

1.2. Detrimental effects of neutrophils in myocardial infarction

Neutrophils have long been considered detrimental in the setting of myocardial injury by contributing to cardiac damage due to their generally pro-inflammatory and cytotoxic functions participating in their role in the defense against invading pathogens (10).

Experimental studies that tried to reduce neutrophil abundance by depletion showed reduced cardiac injury and infarct size (11). Also, clinical studies indicated that neutrophil counts correlated positively with enzymatic and scintigraphic infarct size (12).

Upon stimulation through e.g. cytokines, chemokines or DAMPs, neutrophils release reactive oxygen species (ROS). This process, known as respiratory burst, is mediated by a nicotinamide adenine dinucleotide phosphate dependent pathway. ROS are an effective antimicrobial mechanism but at the same time can directly damage tissue and cells by modifying amino acids, proteins, and lipids and by inducing cytokine and chemokine release (6) (5).

Another main mechanism of neutrophils in protecting their host against pathogen invasion is the release of granule components. Upon degranulation, a wide array of enzymes such as myeloperoxidase (MPO), serine proteases, and matrix metalloproteases (MMP) are released. After MI, MPO is released and it accumulates in the ischemic site to oxidize proteins and lipids (6). Deletion of MPO in a mouse model of MI led to decreased leukocyte infiltration, significant reduction in left ventricular dilation, and marked preservation of left ventricular function (13). Also, MPO has been shown to serve as a major source in the generation of cytotoxic aldehydes, leading to adverse left ventricular dilation and worsened left ventricular function (14) underlying the detrimental effects of MPO in cardiac remodeling.

Serine proteases, including neutrophil elastase, have been shown to be released by neutrophils in the early stages of ischemia, and inhibition of neutrophil elastase led to reduced infarct size (15).

Also, MMPs have been shown to have deleterious effects on cardiac repair after MI by degrading collagen and to lead to worsened left ventricular function (7) (16) (17).

Another specific defense mechanism of neutrophils is the formation of so-called neutrophil extracellular traps (NETs) (5). NETs are structures consisting of decondensed chromatin with granular proteins and cytoplasmic components (18) (19). In clinical studies, NETs have been

shown to be associated with adverse cardiac events, myocardial infarct size, adverse left ventricular remodeling and clinical outcomes (19) (20).

Grune et al. recently showed another deleterious role of neutrophils after MI. In a mouse model, MI combined with hypokalemia triggered arrhythmia as spontaneous ventricular tachycardia. In this model, neutrophils have been shown to promote ventricular arrhythmias, as the depletion of neutrophil lowered the ventricular tachycardia burden compared to mice with regular neutrophil counts. ROS production, especially in non-depleted mice, was enriched in the infarct, relying on high levels of Lipocalin-2, a key neutrophil defense protein. Similarly to depletion of neutrophils, deleting Lipocalin-2 from bone-marrow derived leucocytes reduced the arrhythmia burden (21), thus underlying the detrimental effects of neutrophils in the setting of MI.

1.3. Protective functions of neutrophils in myocardial infarction

Despite the fact that neutrophils have been considered detrimental in the setting of myocardial infarction, increasing evidence shows that neutrophils also play an important role in the resolution of inflammation and thereby in initiating reparative processes necessary for optimal cardiac healing.

Neutrophils are considered professional phagocytes. Therefore, they are involved in clearing the wounds from dead cells, debris and necrotic tissue, which is necessary to prevent persistent pro-inflammatory signals (4).

Neutrophils are the first immune cells to enter the ischemic myocardium after MI (3). After having completed their tasks, they have to be removed from the site of injury, as the persistence of neutrophils can be deleterious and cause chronic inflammation (8). Apoptotic neutrophils produce mediators that attract and recruit macrophages in order to remove them via phagocytosis (22). Phagocytosis of apoptotic neutrophils by macrophages, known as efferocytosis, activates an anti-inflammatory response by producing cytokines such as

transforming growth factor beta (TGF- β) and IL-10 and pro-resolving lipid mediators (23), thereby initiating resolution of inflammation. Inhibition of phagocytosis of apoptotic neutrophils by macrophages promoted left ventricular dilation and mortality (24).

Macrophages show high plasticity in their phenotype, being involved in inflammatory as well as anti-inflammatory and reparative processes which finally lead to scar formation (25). In early phases after MI, macrophages show more pro-inflammatory capacities and polarize toward a pro-reparative phenotype at later time points (26).

In a mouse model of MI, neutrophil depleted mice had worsened cardiac function, increased fibrosis, and progressively developed heart failure. These findings were associated with a lower expression of the phagocytosis receptor myeloid-epithelial-reproductive tyrosine kinase MerTK on macrophages. Further analyses identified that neutrophil gelatinase-associated lipocalin (NGAL) induced the phenotypic shift of macrophages towards a reparative phenotype. This indicates that neutrophils are required for modulating the inflammatory response after MI by polarizing macrophages towards a pro-reparative phenotype (25).

In the reparative phase of the inflammatory response after myocardial infarction, neovascularization is necessary for optimal cardiac repair. It is known that neutrophils are a source of vascular endothelial growth factor (VEGF), a multifunctional cytokine which is essential for mediating neovascularization (27) (9). In transplanted hypoxic tissue, VEGF-A has been shown to be released in high amounts, which led to the recruitment of a proangiogenic subset of CXCR4^{high} neutrophils. This subset carried high amounts of an angiogenic effector protein, Matrix-Metalloprotease-9 (28).

Massena et al. identified a specific subset of neutrophils in mice and humans. These neutrophils stimulated angiogenesis at sites of hypoxia, whereas inhibiting their recruitment to hypoxic tissue impaired neovascularization (29).

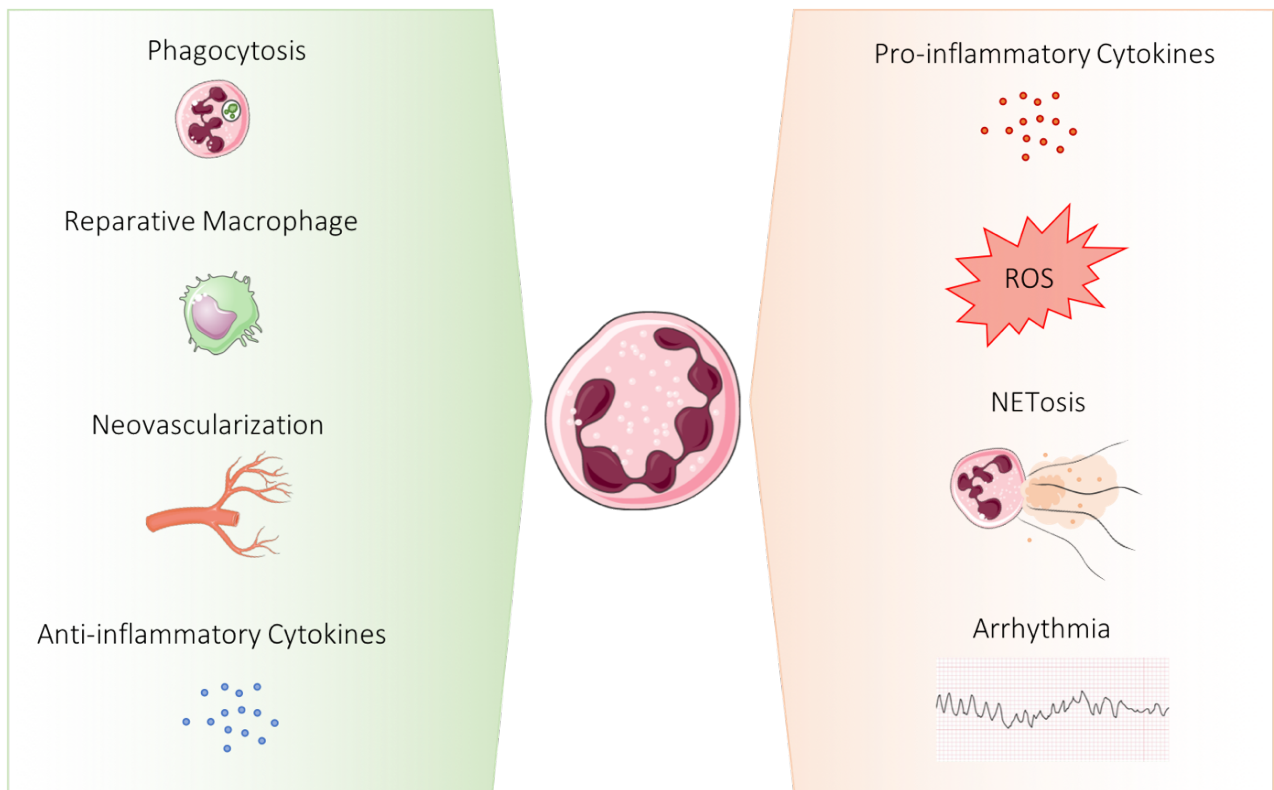


Figure 1.1 Detrimental effects and protective functions of neutrophils in myocardial infarction

Neutrophils play distinct roles in the setting of MI. They have long been considered detrimental due to their pro-inflammatory and defense functions as ROS production, NETosis or production of pro-inflammatory cytokines. Despite this fact, rising evidence shows the important role of neutrophils in the resolution of inflammation and their protective functions in cardiac healing as phagocytosis, stimulation of macrophages towards a pro-reparative phenotype, direct involvement in neovascularization or the release of anti-inflammatory cytokines.

1.4. Neutrophil heterogeneity

The historical view of neutrophils, which considers them a homogeneous population of short-living cells, has been changed. Data from recent years raises evidence that neutrophils show phenotypic and functional heterogeneity, in homeostatic as well as in disease conditions such as acute or chronic inflammation and cancer (30) (31) (32).

In a mouse model of endotoxemia, aged neutrophils have been demonstrated to migrate to the inflammatory site and show higher phagocytosis activity than freshly recruited, non-aged neutrophils. Their higher capacity of phagocytosis depended on specific age-related changes in their molecular pattern, enabling them to serve as “first responders” under inflammatory conditions (33).

In a mouse model of tumors, two different neutrophil subpopulations have been described by Fridlender et al. Tumors were infiltrated with neutrophils characterized by a higher capacity to kill tumor cells, showing increased production of pro-inflammatory cytokines and

hypersegmented nuclei. On the other hand, a second population was identified, showing an immature phenotype and increased arginase activity, thus promoting tumor growth (34).

Focusing on the setting of MI, Ma et al. identified various neutrophil phenotypes that were present in the infarcted area. Neutrophils isolated from ischemic hearts of mice 1 day after MI showed a more pro-inflammatory phenotype. At day 5 and 7 post-MI, neutrophils showed more anti-inflammatory markers (35). Analogously to macrophages, shifting from a pro-inflammatory M1 phenotype in the early phase after MI to an anti-inflammatory M2 phenotype at later stages after MI (36) (2), Ma et al. described these different phenotypes of neutrophils as pro-inflammatory N1 and anti-inflammatory N2. Although N1 neutrophils were always predominant over time, the percentage of anti-inflammatory N2 neutrophils increased after MI. Neutrophils could be polarized to pro-inflammatory N1 in vitro by lipopolysaccharide and interferon- γ or in vivo by DAMPS by activating toll-like receptor-4. On the other hand, anti-inflammatory N2 neutrophils could be polarized in vitro by interleukin-4 (IL-4) (35). Exogenous infusion of IL-4 after MI promotes inflammation resolution by reducing the expression of pro-inflammatory cytokines in neutrophils, as well as stimulating macrophages towards a more reparative phenotype (37).

These results show the high plasticity potential of neutrophils.

Another approach that describes neutrophil heterogeneity performing aptamer proteomics indicated that neutrophils show distinct proteomic profiles over the first days after MI. Neutrophils isolated at day 1 after MI had increased MMP activity. At day 3, neutrophils showed upregulation of apoptosis and induction of extracellular matrix (ECM) organization, which was further increased by neutrophils isolated at day 5 after MI. Neutrophils at day 7 after MI had a reparative signature, which contributed to scar formation (38).

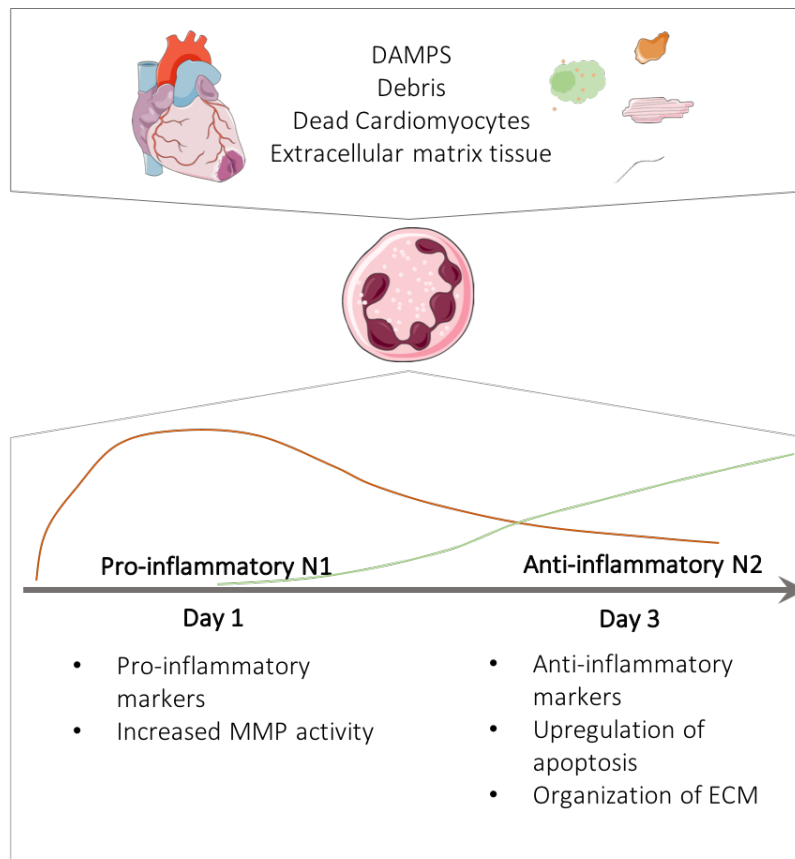


Figure 1.2 Neutrophil heterogeneity in myocardial infarction – polarization from N1 pro-inflammatory towards anti-inflammatory N2 over time

Rising evidence shows that neutrophils display phenotypic and functional differences in the setting of MI. At 1 day after infarction, neutrophils show more pro-inflammatory markers, and polarize towards a more anti-inflammatory state at day 3. Regarding proteomics, neutrophils at day 1 after infarction showed increased MMP activity, whereas neutrophils at day 3 showed upregulation of apoptosis and induction of ECM organization.

Describing neutrophil subsets basically relies on specific phenotypic and functional characteristics such as surface-markers, age or maturity, expression of cytokines or tissue distribution. Distinguishing neutrophil subsets using only phenotypic and functional description is not efficient in describing different states of neutrophils. Also, describing neutrophil heterogeneity in a dichotomic way as either pro- or anti-inflammatory, especially in in vitro experimental settings, simplifies the real changes of neutrophil states in the microenvironment at pathophysiological sites and fails to truly capture the plasticity of neutrophils.

It is necessary to consider proteins together with transcript patterns, functional characteristics and tissue distribution to better understand the dynamics and heterogeneity of neutrophils.

1.5. Preliminary Data

Using new techniques based on single-cell RNA sequencing (scRNA-seq) offers analyzing transcriptomics at single-cell level and recently uncovered new transcriptional states of immune cells in MI (39).

In addition, using oligonucleotide-barcoded antibody labeling before processing cells for scRNA-seq enables the expression of cell-surface markers to be measured at the same time as transcripts expression (40) (41), as well as the processing of several multiplexed biological samples in one single scRNA-seq library (42).

Previous studies by my working group aimed to investigate the dynamics of neutrophil heterogeneity in the ischemic heart. Therefore, single-cell transcriptomics combined with cell surface epitope labeling by sequencing (CITE-seq) was employed in a mouse model of MI.

To analyze transcriptional heterogeneity of neutrophils during the acute phase after MI, heart cell suspensions from 1, 3 and 5 days after MI were compared regarding gene expression patterns at these different time points (fig. 1.3 A, B).

Six transcriptionally distinct clusters of neutrophils were identified (fig. 1.3 C), showing time-dependent appearance and distinct proportions in the ischemic cardiac tissue (fig. 1.3 B, D). At day 1 after MI, cluster Neutro4 (*Cxcl3*, *Lcn2*, *Osm*, *Cd177*, *Ccl6*, *Sell*, *Fpr1*) comprised around 70% of neutrophils, which were almost absent at later time points. At day 3 after MI, cluster Neutro1 was predominant (*Tnf*, *Icam1*, *Il23a*, *Gpr84*). Neutro2 (*Slpi*, *Ifitm1*, *Wfdc17*, *Asprv1*) and represented a cluster which was present at all time points, with increasing proportions from day 1 to day 5. Also, proportions of cluster Neutro3 (*Rps19*, *Ltc4s*, *Nr4a2*) increased over time, showing its highest levels at day 5. Cluster Neutro5 represented a minor cluster with type I interferon response signature (*Isg15*, *Rsad2*, *Ifit1*), and a very minor cluster Neutro6 was characterized by the specific expression of some transcripts (*Psap*, *Slc26a11*, *Gdf15*).

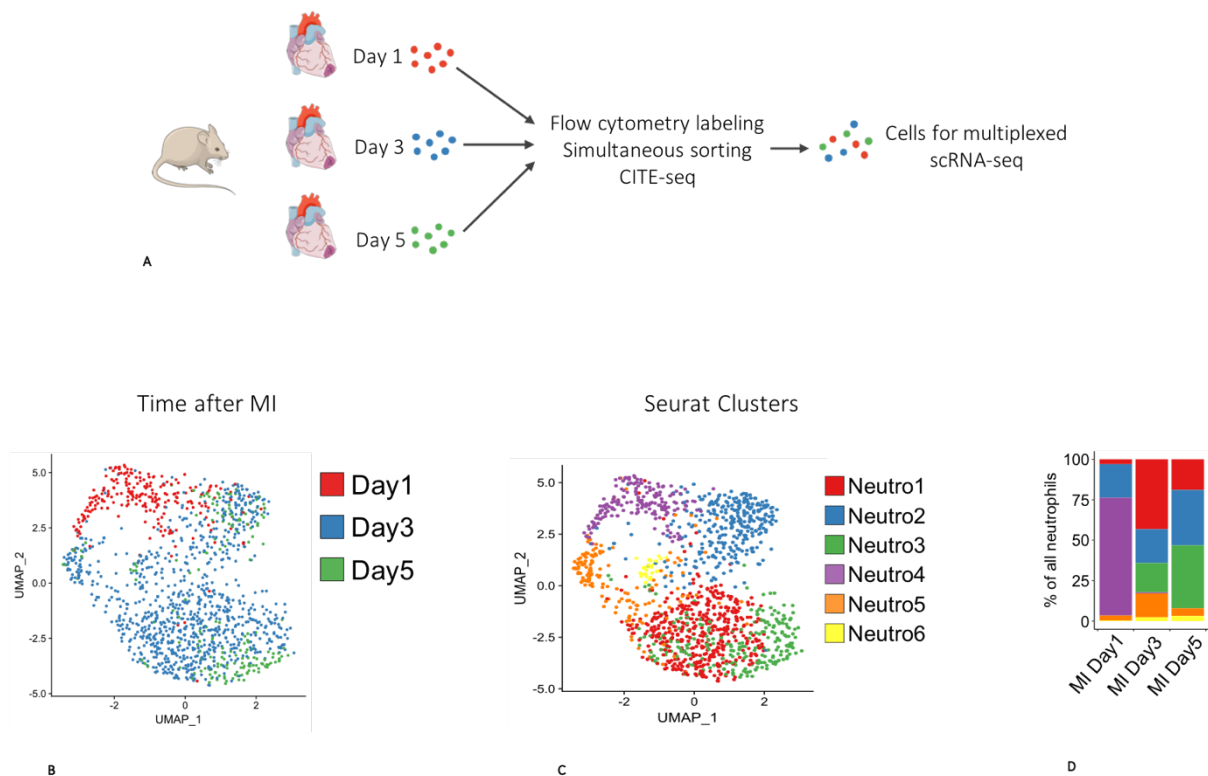


Figure 1.3 scRNA-seq and CITE-seq analysis of cardiac neutrophils 1, 3 and 5 days after myocardial infarction

Courtesy of G. Rizzo, AG Cochain, Universitätsklinikum Würzburg, Experimentelle Biomedizin II

Readapted from Vafadarnejad, Rizzo, Krampert et al. *Circ Res* 2020 (43)

A Graphical overview of the experimental design

B time point of origin of the isolated neutrophils

C Identification of 6 transcriptionally distinct neutrophil clusters

D proportion of each cluster among total neutrophils regarded at each time point

To validate these findings, a separate and independent scRNA-seq experiment was performed, as well as reanalysis of a published scRNA-seq data set of cardiac leucocytes collected 4 days after MI. Altogether, scRNA-seq analysis of cardiac neutrophils pointed out three major time-dependent neutrophil states:

At day 1, neutrophils showed a gene expression pattern typical of bone marrow neutrophils (*Cd177*, *Lcn2*, *Fpr1*), high expression of specific inflammatory cytokines and chemokines (e.g. *Osm*, *Cxcl3*) and activity of transcriptional regulators involved in the hypoxic response (*Hif1a*) and emergency granulopoiesis (*Cebp*). Neutrophils isolated at day 3 and day 5 after MI were characterized by an intermediate or low bone marrow proximity score and were able to be parted into two major subsets of *SiglecF* high (enriched for *Icam1*, *Tnf*) and *SiglecF* low (enriched for *Sipi*, *Ifitm1*) neutrophils (43) (fig. 1.4).

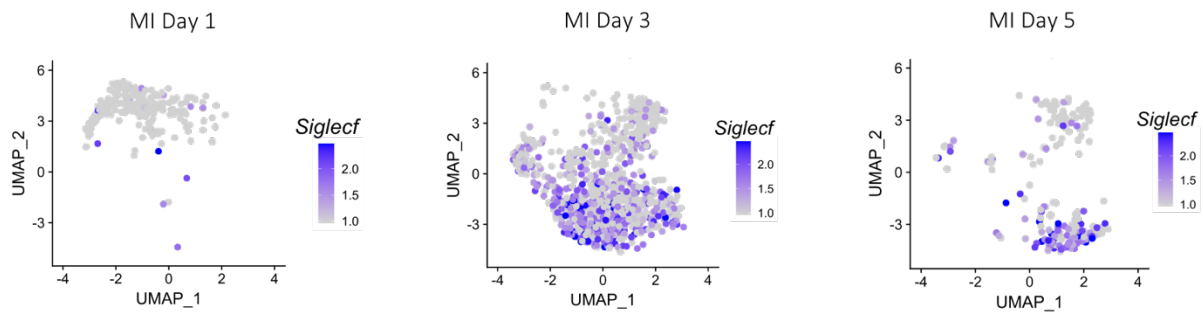


Figure 1.4 Expression of *Siglecf* in isolated neutrophils at different time points
 Courtesy of G. Rizzo, AG Cochain, Universitätsklinikum Würzburg, Experimentelle Biomedizin II
 Readapted from Vafadarnejad, Rizzo, Krampert et al. *Circ Res* 2020 (43)

1.6. Aim of my work

ScRNA-seq analysis of neutrophils isolated from ischemic hearts of mice revealed the time-dependent population of heterogeneous neutrophil clusters with distinct gene expression profiles.

To better understand the dynamics of neutrophil heterogeneity in the ischemic heart, my thesis aimed to address the following points:

Neutrophils isolated at later time points after MI (day 3 and day 5) showed clear enrichment in the expression of *Siglecf* compared to neutrophils isolated at on day 1. By performing flow cytometry analysis, I aimed to validate these findings at the protein level.

The three major neutrophil states after MI were characterized by distinct gene expression patterns. To see whether these distinct subsets of neutrophils show differences in functional characteristics, I aimed to compare their reactive oxygen species (ROS) production and phagocytosis capacity.

As the presence of different neutrophil states was time-dependent, I aimed to modulate circulating neutrophil levels by performing in vivo neutrophil depletion, in order to see how this affects neutrophil subset presence in the ischemic heart.

2. Materials

2.1. Animal model

Name	Company
C57BL6/J	Janvier Labs, France

2.2. Antibodies

FACS			
Name	Color	Clone	Company
CD11b	BV510	M1/70	BioLegend
CD11b	PercpCy5.5	M1/70	BioLegend
CD45	A700	30-F11	BioLegend
CD45	BV650	30-F11	BioLegend
CD64	APC	X54-5/7.1	BioLegend
CD64	A647	X54-5/7.1	BD BioSciences
CD115	APC	AFS98	BioLegend
CXCR2	PeCy7	SA044G4	BioLegend
Ly6G	Pacific Blue	1A8	BioLegend
Ly6G	V450	1A8	BD Biosciences
Ly6G	BV785	1A8	BioLegend
SiglecF	PE	1RNM44N	Thermo Fisher Scientific

SiglecF Immunostaining		
Name	Clone	Company
Alexa 555 goat-anti-rat IgG		Thermo Fisher Scientific
SiglecF rat-anti-mouse	1RNM44N	Thermo Fisher Scientific

In vivo depletion experiments		
Name	Clone	Company
Purified anti-Ly6G <i>in vivo</i> mAb	1A8	BioXCell
Purified Isotype Control	2A3	BioXCell

2.3. General Chemicals and reagents

Name	Company
Collagenase I	Sigma Aldrich
Collagenase XI	Sigma Aldrich
Phosphate Buffered Saline (PBS)	Thermo Fisher Scientific
Dihydrorhodamine 123 (DHR123)	Thermo Fisher Scientific
Erythrocyte lysis buffer	Made in house
Fetal Calf Serum (FCS)	Sigma Aldrich
Fixable Viability Dye e780	Thermo Fisher Scientific
Goat Serum	BioLegend
Hyaluronidase	Sigma Aldrich
Isofluran CP® 1ml/ml	CP-Pharma
Liquid nitrogen	Laboratory's own
Phosphate Buffered Saline	Thermo Fisher Scientific
pHrodo™ Green E. Coli BioParticles™	Thermo Fisher Scientific
RPMI 1640 Medium	Thermo Fisher Scientific
Tissue-Tek® O.C.T™ Compound	Sakura Finetek
VECTASHIELD® mounting medium with DAPI	Vector Laboratories

2.4. Devices

Name	Company
BD FACS Celesta™ Flow Cytometer	BD Biosciences
CM3050 S Cryostat	Leica
Eppendorf® Thermomixer Compact	Sigma Aldrich
Heraeus™ Fresco™ 17 Centrifuge	Thermo Fisher Scientific
Heraeus™ Megafuge™ 40R Centrifuge	Thermo Fisher Scientific
Leica CM3050 S	Leica
Leica DM4000 B LED	Leica Microsystems
Neubauer improved counting chamber	BRAND®
Nikon Eclipse TS100	Nikon
SuperFrost plus slides	Langenbrick GmbH
Sysmex cell count blood	Sysmex
Tissue Disaggregator Plate	SP-ScienceWare Bel-Art

2.5. Software

Name	Version
BD FACSDiva™	10.6
DISKUS Mikroskopische Diskussion	
EndNote	X9.2
FlowJo	10.5.3
GraphPad Prism	7
Microsoft Excel	16.43

3. Methods

3.1. Myocardial infarction model in mice

Myocardial infarction was induced in C57BL6/J mice via permanent ligation of the left anterior descending coronary artery (LAD). To reduce possible effects of gender, age or circadian oscillations on the acute inflammatory response after infarction, all mice were male, 8 to 10 weeks old and underwent surgery between 9:00 and 13:00 o'clock.

Mice preoperatively received an intraperitoneal injection of 0.1 mg/kg body weight Buprenorphine for analgesia.

Anesthesia was induced with inhalation of 4.0% isoflurane; mice were endotracheally intubated and mechanically ventilated with 130 breaths/min and a maximal peak pressure of 18cm H₂O. Anesthesia was maintained with 1.5–2% isoflurane during the surgery.

The thorax was opened in the 4th intercostal space to expose the heart and visually identify the LAD, which was then ligated with a 7/0 non-resorbable nylon suture to induce ischemia in the left ventricle.

Afterwards, the thorax was closed again with four separated 6/0 non-resorbable nylon sutures, the skin was closed continuously with a 6/0 non-resorbable nylon suture.

For postoperative analgesia, the mice received one additional intraperitoneal injection of 0.1 mg/kg body weight Buprenorphine six hours after surgery, as well as twice daily for the following two days after surgery.

The well-being of the mice was monitored regularly using a Score Sheet.

All the animal studies have been approved by the Regierung von Unterfranken, Würzburg, Germany, Aktenzeichen 55.2-DMS-2532-2-743 und Aktenzeichen 55.2-DMS-2532-2-865.

3.2. Exclusion criteria

Mice that died because of myocardial infarction before being sacrificed for experiments were excluded from analysis. Further specific exclusion criteria were the absence of visually detectable myocardial infarction, as well as an infarct that comprised visually less than around 30% of the left ventricle.

3.3. Cell isolation

3.3.1. Enzymatic processing of the heart for cell isolation

The mice were anesthetized with 4.0% isoflurane inhalation and sacrificed by cervical dislocation. The thorax and diaphragm were opened to expose the heart and visually verify myocardial infarction. The vena cava inferior was cut before perfusing the heart with PBS to wash out the blood. Afterwards, the heart was taken out. The right ventricle and healthy cardiac tissue above the ligation were removed to further process only infarcted cardiac tissue and the infarct border zone. In one experiment, we further processed the remote part of the peri-infarcted area of the left ventricle for separate analyses, the so-called remote area. A similar part of the left ventricle was taken out of sham operated control mice without permanent ligation of the LAD for further processing.

The heart was washed in RPMI to remove leftover blood and was then transferred into a 1.5mL microtube and minced with surgical scissors. The heart pieces were enzymatically digested in 1mL RPMI containing a final concentration of 450 U/mL Collagenase I, 125 U/mL Collagenase XI and 60 U/mL Hyaluronidase, incubating in a Thermomixer at 37°C with shaking set at 1000rpm for 1 hour.

Afterwards, the digested cell suspension was filtered through a 70µm cell strainer, dissociating leftover undigested pieces with a syringe plunger.

The suspension was then centrifuged in 30mL PBS containing 1% FCS for 5 minutes at 400g and 4°C. After removing the supernatant, the cell pellet was resuspended in PBS containing 1% FCS.

3.3.2. Mechanical processing of the heart for cell isolation

Previous experiments showed that epitopes such as CXCR2 are affected by enzymatic processing of the heart. Therefore, another method to digest cardiac tissue mechanically was established to obtain fresh neutrophils for functional assays.

Mice were sacrificed and their hearts taken out as described above. The heart was transferred into a 1.5mL microtube filled with PBS containing 1% FCS and minced with surgical scissors. The pieces were mechanically dissociated using a Tissue Disaggregator plate. The cell suspension was then directly filtered through a 70µm cell strainer, dissociating leftover pieces with a

syringe plunger, and centrifuged in a large volume of 50mL of PBS containing 1% FCS for 5 minutes at 300g and 4°C. After removing the supernatant, the cell pellet was resuspended in PBS containing 1% FCS.

3.3.3. Processing of the bone marrow for cell isolation

Mice were sacrificed as described above. One leg was dissected to take out the femur, which had been completely cleaned of all muscles. The knee part of the femur was removed in order to put it with the opening down in a 1mL microtube with a perforated bottom, which was then transferred into a 1.5mL microtube. It was centrifuged for 20 seconds at 10000g to centrifuge the bone marrow out of the femur into the 1.5mL microtube. The cell pellet was resuspended in 1mL PBS containing 1% FCS (44).

3.3.4. Processing of the blood for cell isolation

Mice were sacrificed as described above. After the thorax and diaphragm were opened and the heart exposed, blood was collected in EDTA-coated tubes by puncturing the right ventricle. 150µL was transferred into a 1.5mL microtube and supplemented with an 850µL erythrocyte lysis buffer and incubated for 10 minutes at 4°C to lyse erythrocytes. The suspension was centrifuged for 5 minutes at 400g and 4°C. After the supernatant had been aspirated, the cell pellet was resuspended in 250µL PBS containing 1% FCS.

3.3.5. Processing of the spleen for cell isolation

Mice were sacrificed as described above. The spleen was taken out and dissociated through a 70µm cell strainer using a syringe plunger. The cell strainer was washed with 5mL PBS containing 1% FCS to collect all the cells. The suspension was then centrifuged for 5 minutes at 400g and 4°C, and after removing the supernatant resuspended in 3mL of erythrocyte lysis buffer and incubated for 7 minutes at room temperature to remove erythrocytes.

After incubation, 7mL of PBS containing 1% FCS were added and the suspension was centrifuged again for 5 minutes at 400g and 4°C. After the supernatant had been removed, the cells were resuspended in 10mL PBS containing 1% FCS and filtered once again through a 70µm cell strainer.

3.4. Organ freezing and immunohistological staining

3.4.1. Organ freezing and preparation of cryosections

Mice that had undergone permanent ligation of the LAD were sacrificed at either day 1 or day 3 after myocardial infarction. The heart was injected with PBS containing 10% KCl to arrest it in diastole. Before being taken out, the heart was flushed with PBS containing 1% FCS to wash out the blood.

The right ventricle was removed, and the heart was mounted on a cork plate by using Tissue-Tek OCT compound to cover it completely before freezing it in liquid nitrogen cooled 2-Methylbutane. To cut cross-sections, we used the Leica CM3050 S Cryostat at -20°C. The heart was cut into 7µm cryosections on SuperFrost Plus section slides which were stored in a -80°C freezer until used for immunohistological staining.

3.4.2. Immunohistological staining and imaging

3.4.2.1. *SiglecF staining*

Sections were washed in PBS for 10 minutes to remove Tissue-Tek OCT. To block non-specific antibody binding, sections were first incubated with 10% normal goat serum for 20 minutes. After having been washed, sections were incubated for 2 hours with rat anti-mouse SiglecF antibody in a final concentration of 10µg/mL, or with the appropriate isotype antibody to obtain a negative control test. After another washing step, sections were incubated with goat anti-rat Alexa555 secondary antibody (dilution 1/300) for 1 hour.

After a last washing step, sections were mounted with DAPI-containing Vectashield medium and coverglass. All incubation steps were conducted in a humidified chamber.

3.4.2.2. *Fluorescence microscopy imaging*

Fluorescence microscopy imaging was carried out with the Leica DM4000 B LED Fluorescence microscope and the DISKUS software.

3.5. Cell counting

For processed cell suspensions of heart, bone marrow and spleen, the number of cells was determined using the Neubauer counting chamber. Diluted cell suspensions were counted using a light microscope (magnification) in at least 2 of the 4 squares of the counting chamber to obtain a mean value of the counted sum of cells. The number of cells per mL was then calculated using the following formula:

$$\text{number of counted cells} \times \text{dilution factor} \times 10^4$$

For processed cell suspensions of the blood, the number of cells was counted using a Sysmex cell counting blood.

3.6. Flow cytometry

3.6.1. Fluorescence activated cell sorting FACS

For our experiments we used a BD FACS Celesta™ flow cytometer and analyzed data with FlowJo.

3.6.2. Staining of surface markers

Organs were processed for cell isolation as described above. After the last washing step and resuspension in PBS containing 1% FCS, a maximum of 10^6 cells per well were plated in a 96 round-bottom plate. Cells were centrifuged for 5 minutes at 400g and 4°C. After discarding the supernatant, the cells were resuspended in 10µg/mL purified rat anti-mouse antibody (TruStain FcX BioLegend) for 10 minutes at 4°C to block non-specific binding of antibodies against FC receptors. Cells were then incubated with Fixable Viability Staining e780 and fluorochrome coupled antibodies against the following surface markers, employed at concentrations recommended by the manufacturer.

Fluorochrome-conjugated antibodies for surface labeling of neutrophils in enzymatically digested heart, blood, bone marrow and spleen cell suspensions for flow cytometry

Antibody	Fluorochrome	Dilution
CD45	BV650	1/300
CD11b	PercpCy5.5	1/300
Ly6G	Pacific Blue	1/300
SiglecF	PE	1/100

Fluorochrome-conjugated antibodies for surface labeling of neutrophils in mechanically digested heart cell suspensions for flow cytometry

Antibody	Fluorochrome	Dilution
CD45	A700	1/400
CD11b	PercpCy5.5	1/300
CD11b	BV510	1/100
CD64	APC	1/100
CD64	A647	1/100
CXCR2	Pe-Cy7	1/100
Ly6G	BV785	1/300
Ly6G	Pacific Blue	1/300
Ly6G	V450	1/300
SiglecF	PE	1/100

Fluorochrome-conjugated antibodies for surface labeling of neutrophils in mechanically digested heart cell suspensions for ROS production activity assay

Antibody	Fluorochrome	Dilution
Ly6G	BV785	1/300
SiglecF	PE	1/100

Fluorochrome-conjugated antibodies for surface labeling of neutrophils in mechanically digested heart cell suspensions for phagocytosis activity assay

Antibody	Fluorochrome	Dilution
Ly6G	BV785	1/300
SiglecF	PE	1/100

Fluorochrome-conjugated antibodies for surface labeling of neutrophils in mechanically digested heart, blood, bone marrow and spleen cell suspensions for neutrophil depletion experiments

Antibody	Fluorochrome	Dilution
CD115	APC	1/300
CD11b	PercpCy5.5	1/300
CD11b	BV510	1/100
CD45	A700	1/400
CD64	APC	1/100
CXCR2	PE-Cy7	1/100
Ly6G	BV785	1/300
Ly6G	Pacific Blue	1/300
SiglecF	PE	1/100

3.7. Neutrophil activity assays

3.7.1. ROS production activity assay

To examine differences between neutrophil subpopulations in the production of reactive oxygen species, cell suspensions were incubated with dihydrorhodamine (DHR) 123. DHR123 is a probe that can passively enter cells. Upon stimulation, it indicates superoxide formation when it is oxidized by H₂O₂ to the fluorescing derivate rhodamine localized in mitochondria. These fluorescing derivatives can be detected via flow cytometry (fig. 3.1).

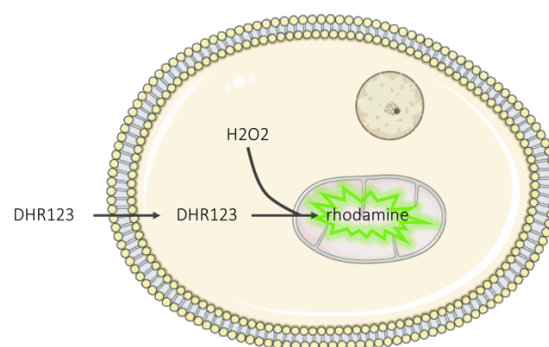


Figure 3.1 Chart of ROS production activity assay

Cells from ischemic hearts were collected 1 and 3 days after myocardial infarction and processed for flow cytometry labeling, as described above.

The cell suspension was incubated for 30 minutes at 4°C with Fixable Viability Staining e780 and fluorochrome-conjugated antibodies against Ly6G (BV785) and SiglecF (PE).

The cells were always kept on ice to avoid production of reactive oxygen species before stimulation.

After washing, the cells were resuspended in DHR123 (dilution 1/200) and incubated for 30 minutes at 37°C. After incubation, the cells were washed and resuspended in PBS 1% FCS and analyzed via flow cytometry.

Data was acquired using a BD FACS Celesta™ flow cytometer and analyzed with FlowJo.

Neutrophils were gated as living, Ly6G⁺ and SiglecFlow or SiglecF^{high} cells.

To obtain reliable results for differences in ROS production activity in neutrophil subpopulations, fluorescence intensity in each subpopulation was analyzed, and the geometric mean of light emitted from the fluorescing derivatives in the green channel (FITC), which relies on the amount of reactive oxygen species produced, was compared.

3.7.2. Phagocytosis activity assay

To compare phagocytosis activity between different neutrophil subpopulations, pHrodo™ Green *E. coli* BioParticles® Conjugate was used, a pH-sensitive dye that indicates phagocytosis by increasing fluorescence intensity in more acidic surroundings, such as in phagosomes (fig. 3.2).

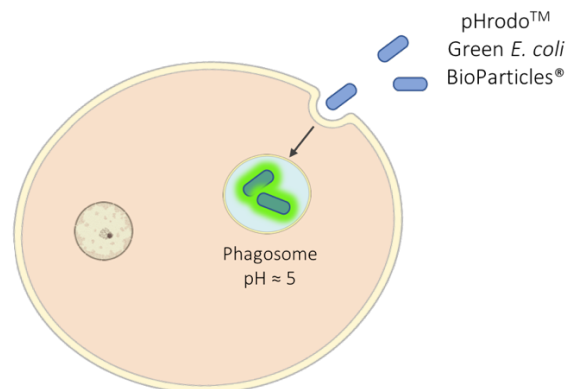


Figure 3.2 Chart of phagocytosis activity assay

Cells from ischemic hearts were collected 1 and 3 days after myocardial infarction or from non-infarcted control mice and processed for flow cytometry labeling, as described above.

pHrodo™ Green *E. coli* BioParticles® Conjugate was reconstituted in a 1 mg/mL solution in RPMI.

Cells were incubated with *E. coli* BioParticles® for 30 minutes at 37°C in a final concentration of 10 µg/mL to stimulate phagocytosis, or without bioparticles to obtain a negative control (FMO). After washing with PBS 1% FCS, samples were incubated for 30 minutes at 4°C with Fixable Viability Staining e780 and fluorochrome conjugated antibodies against Ly6G (BV785) and SiglecF (PE). After incubation, the cells were washed and resuspended in PBS 1% FCS and analyzed via flow cytometry.

Data was acquired using a BD FACS Celesta™ flow cytometer and analyzed with FlowJo.

Neutrophils were gated as living, Ly6G+ cells. Neutrophils isolated from 3-day-old infarcted hearts were furthermore distinguished between in terms of SiglecF^{high} and SiglecF^{low}-expressing neutrophils.

To analyze quantitative differences in phagocytosis activity between neutrophil subpopulations, the percentage of cells that showed phagocytosis activity in each experimental group was compared.

3.8. In vivo depletion of neutrophils to investigate time-dependent roles and functional impacts of neutrophil subpopulations

Depletion of neutrophils facilitates investigating changes in neutrophil heterogeneity and their functional effect in the ischemic heart depending on their temporal appearance after infarction and the onset of depletion.

To better understand the time-dependent role and functional differences between neutrophil subpopulations, antibody-mediated in vivo depletion experiments in mice with myocardial infarction were performed.

A previously published protocol for neutrophil depletion in mouse myocardial infarction was followed using anti-Ly6G antibodies (25). Mice were divided into different groups, receiving 1 i.p. injection of 50 μ g of anti-Ly6G antibodies per day to deplete circulating neutrophils consistently. Depending on the group, the i.p. injection started either at day 1 before myocardial infarction, or at day 1 or day 2 after myocardial infarction and was continued until all groups of mice were sacrificed at day 3 after myocardial infarction. To obtain a negative control, one group of mice didn't receive any injection of anti-Ly6G antibodies. Instead, they received the appropriate isotype control antibody.

To reproduce our findings, a validation experiment for neutrophil depletion was performed. Results from 1 day after myocardial infarction as well as 3 days after myocardial infarction were compared.

Organs were harvested and processed as described above to isolate cells for flow cytometry analyses.

Data on each processed cell suspension from all organs was acquired using a BD FACS Celesta™ flow cytometer and analyzed with FlowJo.

To verify successful depletion of neutrophils, two established gating strategies were performed on each sample analyzed.

First, neutrophils were gated based on the surface marker Ly6G.

Neutrophils from enzymatically and mechanically digested ischemic hearts were identified as CD45+CD11b+CD64-Ly6G+ cells. Blood, bone marrow and spleen neutrophils were identified using the same gating strategy.

Then, the results were compared with findings by gating neutrophils based on CXCR2. Neutrophils from mechanically digested ischemic hearts were identified as CD45+CD11b+CD64-CXCR2+ cells. CD64 served as an exclusion marker, as it is only expressed on monocytes and macrophages, but not neutrophils. Blood and spleen neutrophils were identified using the same gating strategy. Bone marrow neutrophils were identified as CD45+CD11b+CD115-Ly6G+ or CD45+CD11b+CD115-CXCR2+ cells. Here, CD115 served as an exclusion marker for monocytes.

3.9. Calculations and statistical analyses

All calculations were done with Excel v16.43.

Statistical analyses were performed using GraphPad Prism v7. Data was first subjected to the D'Agostino / Pearson normality test.

In multiple group analyses that were normally distributed after the D'Agostino / Pearson normality test, data was further analyzed with the parametric one-way ANOVA test followed by Tukey's test for multiple comparison.

In multiple group analyses that were non-normally distributed, data was further analyzed with the non-parametric Kruskal-Wallis test followed by Dunn's multiple comparison test.

In 2 group analyses, a Student's test for normally distributed data was performed. For non-normally distributed data, data from 2 group experiments were analyzed with a Mann-Whitney U test.

4. Results

4.1. Appearance of SiglecF+ neutrophils in the infarcted heart at day 3 post-MI

Results from preliminary scRNAseq experiments by my working group showed clear differences in gene expression patterns between distinct neutrophil clusters at different time points after MI. One noticeable finding was the clear difference between transcript levels of *SiglecF* in neutrophils isolated from ischemic hearts at different time points.

Indeed, neutrophils isolated at day 3 after myocardial infarction showed much higher transcript levels of *SiglecF* compared to neutrophils isolated at day 1 after MI (43).

To verify these findings at the protein level, ischemic and control hearts from male mice were analyzed by performing flow cytometry of enzymatically digested hearts. Hearts, blood, bone marrow and spleens were processed and analyzed from mice 1 day and 3 days after the onset of cardiac ischemia. To analyze the influx of inflammatory cells in the direct environment of the infarcted tissue, the peri-infarcted remote area of the same hearts was also processed and analyzed. Sham operated mice, as well as mice without any operation, served as negative controls. All cohorts of mice were sacrificed, and their organs were processed and analyzed the same day to ensure identical experimental conditions. Neutrophils were gated as viable CD45+CD11b+Ly6G+ cells (fig. 4.1).

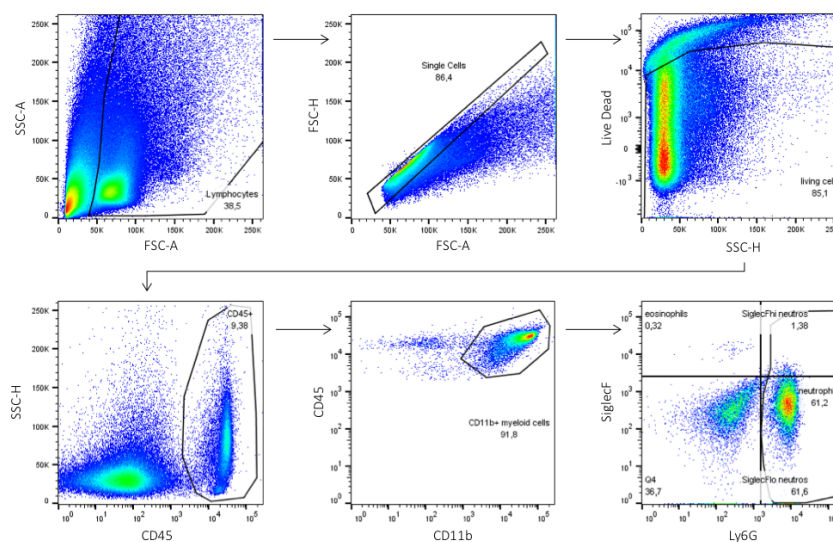


Figure 4.1 Gating strategy of cardiac neutrophils

Cells identified as SSC-A and FSC-A positive. Removal of doublets by gating single cells. Exclusion of dead cells by gating living cells as e780-. Gating leucocytes as CD45+. Gating myeloid cells as CD45+CD11b+. Identification of neutrophils gated as CD45+CD11b+Ly6G+ cells. Defining SiglecFhigh and SiglecFlow neutrophils by gating eosinophils as CD45+CD11b+Ly6G- cells.

At day 1 after infarction, neutrophil infiltration peaked at $49.4 \pm 11.3\%$ of CD45⁺ cells and decreased to $29.3 \pm 6.9\%$ of CD45⁺ cells at day 3 after MI. In the remote area, hearts 1 day after MI also had higher counts of neutrophils compared to hearts 3 days after MI, but at both time points neutrophil counts were significantly lower than in the ischemic area. In sham operated control mice, only a low number of neutrophils could be detected. The detection of neutrophils in sham samples could possibly be due to inflammatory responses after sham surgery (fig. 4.2).

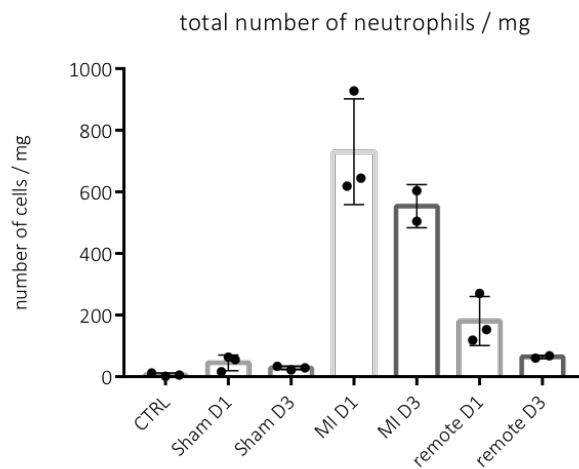


Figure 4.2 Total number of cardiac neutrophils in the different cohorts.

Total number of neutrophils among total CD45⁺ leukocytes in the cardiac tissue at different time points after myocardial infarction. CTRL: no infarction controls. Sham D1: sham operated mice 1 day after surgery. Sham D3: sham operated mice 3 days after surgery. MI D1: mice 1 day after myocardial infarction. MI D3: mice 3 days after myocardial infarction. Remote D1: periinfarcted cardiac tissue 1 day after myocardial infarction. Remote D3: periinfarcted cardiac tissue 3 days after myocardial infarction.

As SiglecF is a known surface molecule on eosinophils (45) (46), the gate for SiglecF^{high}-expressing neutrophils (SiglecF^{high}) was defined by gating eosinophils (fig. 4.1), which were identified as CD45⁺CD11b⁺Ly6G⁻SiglecF⁺ cells and based on their SSC/FSC properties (SSC^{high}) (fig. 4.3). Ly6G⁺SiglecF^{high} and Ly6G⁺SiglecF^{low} neutrophils were SSC intermediate, corroborating these cells as being neutrophils (fig. 4.3).

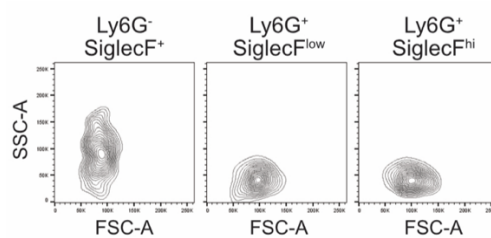


Figure 4.3 Side scatter (SSC)-A / Forward scatter (FSC)-A properties of Ly6G⁻SiglecF⁺ eosinophils, Ly6G⁺SiglecF^{low} and Ly6G⁺SiglecF^{high} neutrophils

Eosinophils identified as CD45⁺CD11b⁺Ly6G⁻SSC^{high}. Ly6G⁺SiglecF^{low} and Ly6G⁺SiglecF^{high} neutrophils identified as SSC^{intermediate}.

At day 3 after MI, $57.1 \pm 2.4\%$ of all isolated Ly6G⁺ neutrophils were SiglecF^{high}. Compared to this, only $3.1 \pm 2.1\%$ of Ly6G⁺ neutrophils isolated from ischemic hearts at day 1 after infarction expressed SiglecF ($P < 0.0001$) (fig. 4.4 A, B). There was also a small difference in SiglecF^{high} neutrophils in the remote areas, increasing from $5.1 \pm 4.4\%$ at day 1 up to $11.1 \pm 2.7\%$ at day 3 (fig. 4.4 B).

Control mice as well as sham operated mice didn't show any significant increase in SiglecF^{high} neutrophils between day 1 and day 3 after infarction (fig. 4.4 B).

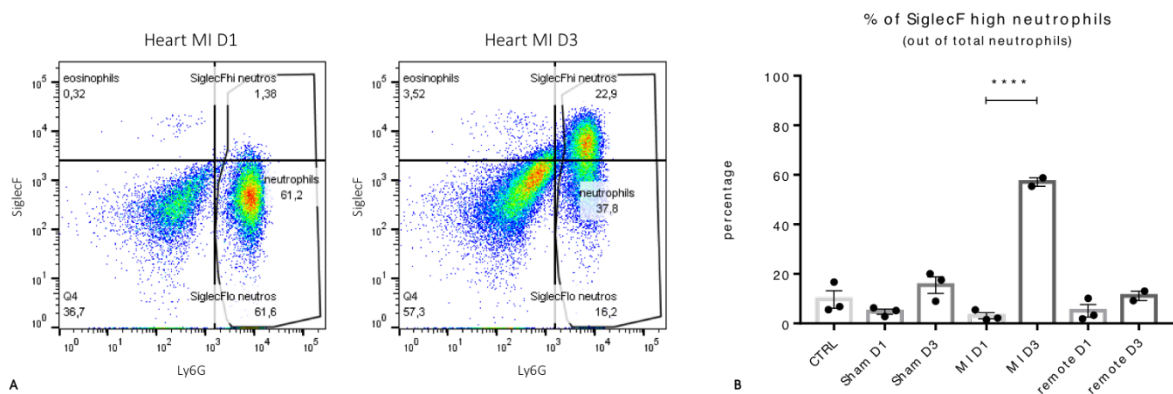


Figure 4.4 Proportion of SiglecF^{high} neutrophils among total cardiac neutrophils

A Representative example of a FACS dot plot of SiglecF^{high} cardiac neutrophils 1 day and 3 days after myocardial infarction.

B Percentage of SiglecF^{high} cardiac neutrophils in experimental cohorts. **** $p < 0.0001$

4.2. Absence of SiglecF^{high} neutrophils in bone marrow, blood and spleens

SiglecF^{high} neutrophils were mainly present in ischemic hearts at day 3 after MI and nearly absent at day 1 after infarction. One possible reason for this could be that SiglecF^{high} neutrophils are produced within the bone marrow during emergency granulopoiesis as a response to myocardial infarction, released into the blood to then infiltrate the ischemic heart and, therefore, are only present at later time points after myocardial infarction. To verify this hypothesis, neutrophils from bone marrow, blood and spleens were analyzed and the expression of SiglecF between day 1 and day 3 after myocardial infarction was compared.

4.2.1. Absence of SiglecF^{high} neutrophils in the bone marrow

Neutrophils were gated as viable CD45+CD11b+Ly6G+ cells. As expected, there were nearly no SiglecF^{high} neutrophils in the bone marrow isolated from mice 1 day after MI, which represented $0.5 \pm 0.1\%$ of total neutrophils (fig. 4.5 A, B).

Interestingly, there was not any increase in SiglecF^{high} neutrophils in the bone marrow at day 3 after MI, which still constituted only $0.7 \pm 0.3\%$ of the total neutrophils (fig. 4.5 A, B). Neutrophils from control as well as from sham operated mice did not show any difference in SiglecF^{high} neutrophil proportions between day 1 and day 3 after MI (fig. 4.5 B).

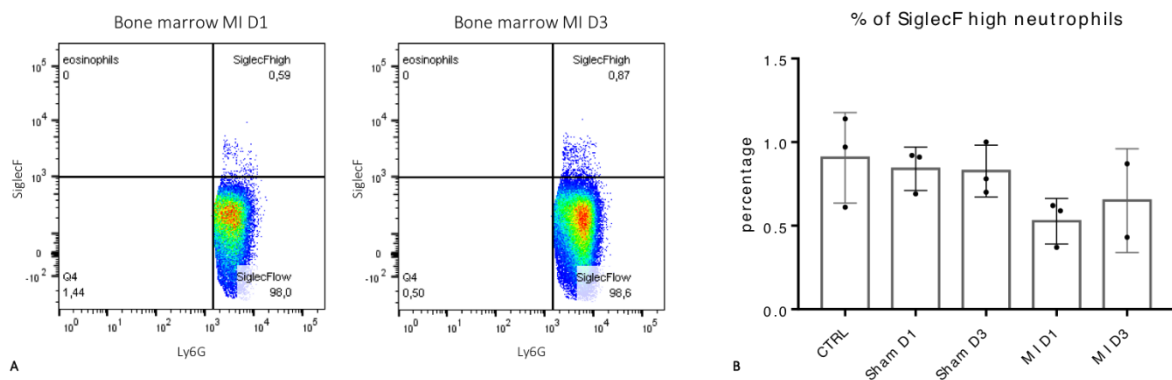


Figure 4.5 Proportion of SiglecF^{high} neutrophils among total bone marrow neutrophils

A Representative example of a FACS dot plot of SiglecF^{high} bone marrow neutrophils 1 day and 3 days after myocardial infarction.

B Percentage of SiglecF^{high} bone marrow neutrophils in experimental cohorts.

4.2.2. Absence of SiglecF^{high} neutrophils in the blood

Neutrophils were gated as viable CD45+CD11b+Ly6G+ cells. At day 1 after infarction, SiglecF^{high} neutrophils constituted $0.9 \pm 0.1\%$ of the total neutrophils, and this proportion did not increase at day 3 after infarction, constituting $1.4 \pm 0.8\%$ of the total neutrophils (fig. 4.6 A, B).

Neutrophils from control as well as from sham operated mice did not show any difference in SiglecF^{high} neutrophil proportions between day 1 and day 3 after MI (fig. 4.6 B).

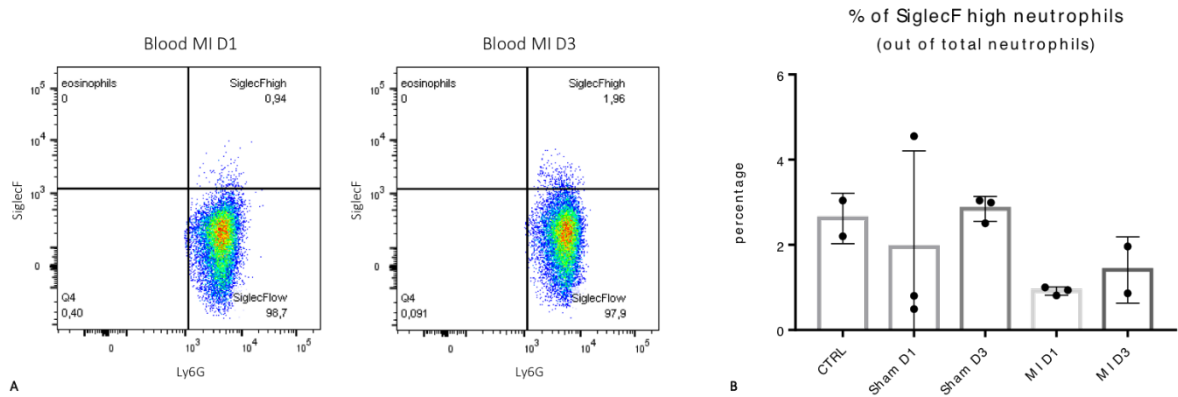


Figure 4.6 Proportion of SiglecFhigh neutrophils among total blood neutrophils

A Representative example of a FACS dot plot of SiglecFhigh blood neutrophils 1 day and 3 days after myocardial infarction.

B Percentage of SiglecFhigh blood neutrophils in experimental cohorts.

4.2.3. Absence of SiglecFhigh neutrophils in the spleen

Neutrophils were gated as viable CD45+CD11b+Ly6G+ cells. At day 1 after MI, SiglecFhigh neutrophils constituted $1.0 \pm 0.3\%$ of total neutrophils. At day 3 after MI, SiglecFhigh neutrophils did not increase significantly, still representing only $2.1 \pm 1.1\%$ of the total neutrophils (fig. 4.7 A, B).

Neutrophils from control as well as from sham operated mice did not show any difference in SiglecFhigh neutrophil proportions between day 1 and day 3 after MI (fig. 4.7 B).

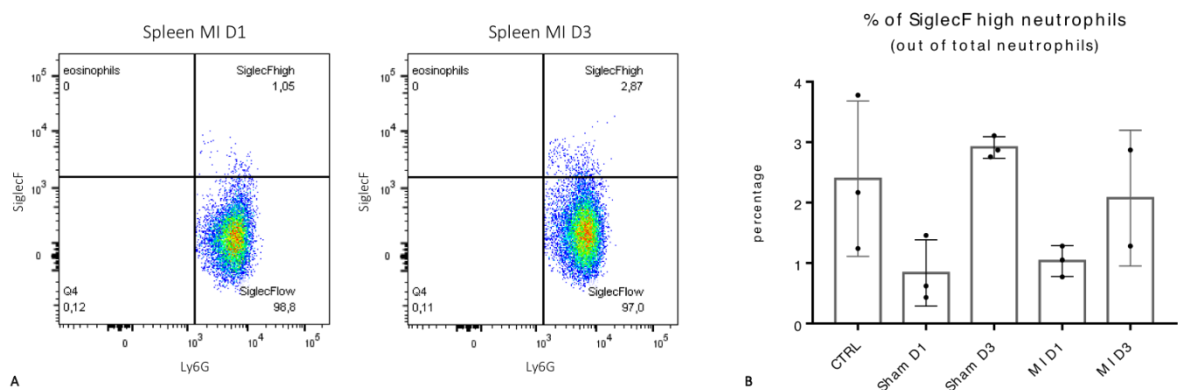


Figure 4.7 Proportion of SiglecFhigh neutrophils among total spleen neutrophils

A Representative example of a FACS dot plot of SiglecFhigh spleen neutrophils 1 day and 3 days after myocardial infarction.

B Percentage of SiglecFhigh spleen neutrophils in experimental cohorts.

4.3. Validation experiment

A similar experiment was repeated with a higher number of mice to reproduce and verify these findings. Ischemic and no infarction control hearts from male mice were mechanically digested and analyzed by performing flow cytometry.

Hearts and blood were processed and analyzed from mice 1 day and 3 days after the onset of ischemia.

4.3.1. Heart

Neutrophils were gated as described above.

Total numbers of neutrophils peaked at day 1 after myocardial infarction, representing $48.0 \pm 5.5\%$ of CD45+ cells, while becoming lower at day 3, representing $36.4 \pm 7.0\%$ of CD45+ cells ($P = 0.0156$ MI D1 versus MI D3) (fig. 4.8).

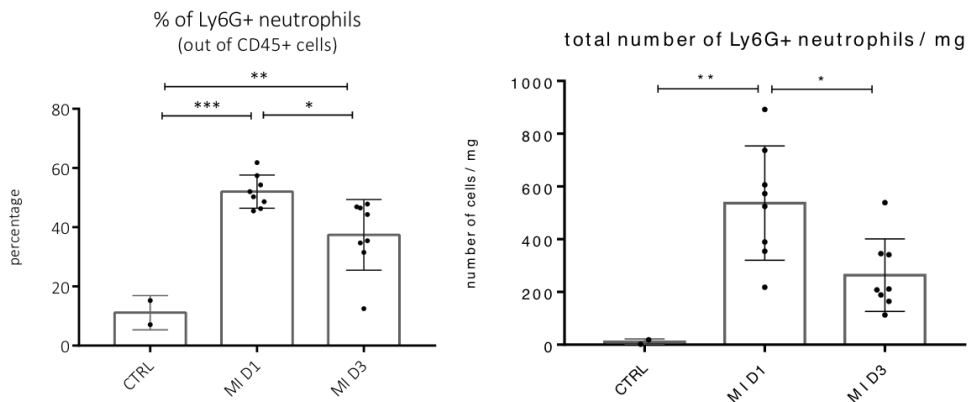


Figure 4.8 Proportion and total number of cardiac neutrophils in the different cohorts

Proportion and total number of neutrophils among total CD45+ leukocytes in the cardiac tissue 1 and 3 days after myocardial infarction and no infarction control hearts.

CTRL: no infarction controls. MI D1: mice 1 day after myocardial infarction. MI D3: mice 3 days after myocardial infarction.

* $p < 0.05$; ** $p < 0.01$; *** $p < 0.001$

Proportion of SiglecFhigh neutrophils increased from day 1 to day 3 after myocardial infarction, representing $4.1 \pm 1.5\%$ of total neutrophils at day 1 compared to $38.0 \pm 10.0\%$ of the total neutrophils at day 3 ($P = 0.0123$ MI D1 versus MI D3) (fig. 4.9), thus corroborating results from the previous experiment.

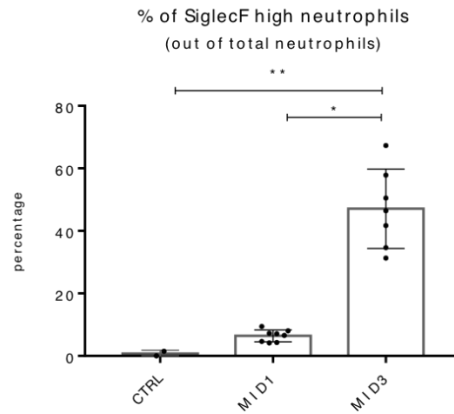


Figure 4.9 Proportion of SiglecFhigh neutrophils among total cardiac neutrophils

Proportion of SiglecFhigh neutrophils among total neutrophils in the cardiac tissue 1 and 3 days after myocardial infarction. CTRL: no infarction controls. MI D1: mice 1 day after myocardial infarction. MI D3: mice 3 days after myocardial infarction. * $p < 0.05$; ** $p < 0.01$

4.3.2. Blood

Neutrophils were gated as described above. There was no significant change in SiglecF expression to observe on neutrophils isolated at day 1 after infarction (SiglecFhigh neutrophils representing $0.6 \pm 0.3\%$ of the total neutrophils) compared to neutrophils isolated at day 3 (SiglecFhigh neutrophils representing $1.3 \pm 0.6\%$ of the total neutrophils) (fig. 4.10).

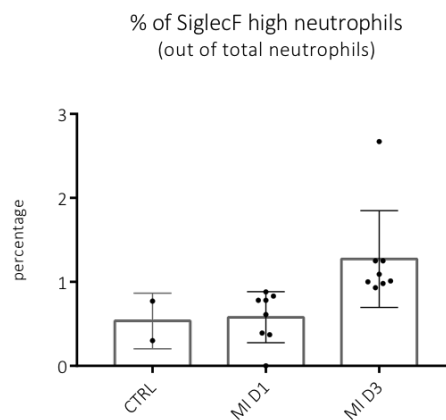


Figure 4.10 Proportion of SiglecFhigh neutrophils among total blood neutrophils

Proportion of SiglecFhigh neutrophils among total neutrophils in the blood 1 and 3 days after myocardial infarction. CTRL: no infarction controls. MI D1: mice 1 day after myocardial infarction. MI D3: mice 3 days after myocardial infarction.

Altogether, these results show that SiglecF^{high} neutrophils are only present in ischemic hearts 3 days after the onset of myocardial infarction, which indicates that the expression of SiglecF may be only acquired locally in the ischemic heart tissue.

4.4. Immunofluorescence localization of SiglecF⁺ cells in the infarcted area

SiglecF⁺ neutrophils are enriched in ischemic hearts mainly at day 3 after myocardial infarction. To see where exactly these SiglecF⁺ neutrophils are localized, immunohistological staining was performed on cryosections of freshly frozen infarcted hearts at day 1 and day 3 after MI.

SiglecF⁺ cells were only present in the infarcted area and its border zone, which was visually identified by a thinner wall and degraded cardiomyocytes.

In sections of ischemic hearts at day 3 after MI, SiglecF⁺ neutrophils could be detected in all the infarcted area, whereas nearly no SiglecF⁺ neutrophils could be visualized in hearts at day 1 after infarction (fig. 4.11), thus confirming the results from flow cytometry analyses.

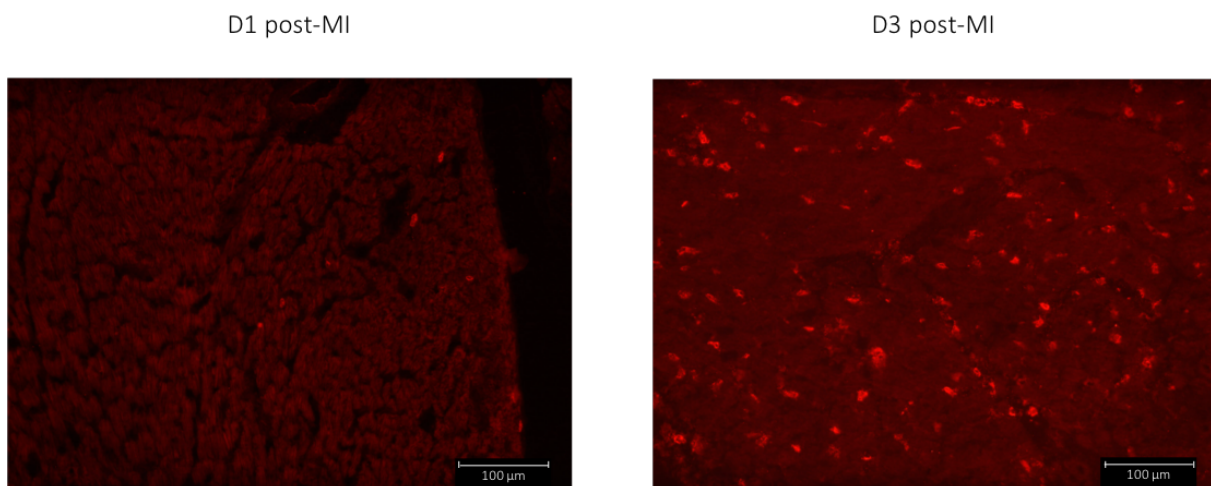


Figure 4.11 Immunofluorescence localization of SiglecF⁺ cells. Immunohistological staining of SiglecF⁺ cells on freshly frozen infarcted hearts 1 and 3 days after myocardial infarction.

4.5. Cardiac neutrophil subsets show differences in major functional capacities

The previous results showed clear time-dependent differences in the presence of different neutrophil subpopulations in the heart. To investigate whether these subpopulations could also be specialized in major neutrophil functions, a comparison of reactive oxygen species (ROS) production and phagocytosis activity between these subpopulations was performed.

4.5.1. Phagocytosis

Mice with myocardial infarction were sacrificed at either day 1 or day 3 after infarction. Processed heart cell suspensions were incubated with a solution of PHrodo™ Green *E. coli* BioParticles® Conjugate in a final concentration of 10µg/mL or without PHrodo™ Green *E. coli* BioParticles® Conjugate to serve as a negative control (FMO Control). Neutrophils isolated from hearts 1 or 3 days after MI were gated as living, Ly6G+ cells. Neutrophils from 3-day-old infarcted hearts were furthermore distinguished between in terms of SiglecF^{high} and SiglecF^{low} neutrophils (fig. 4.12).

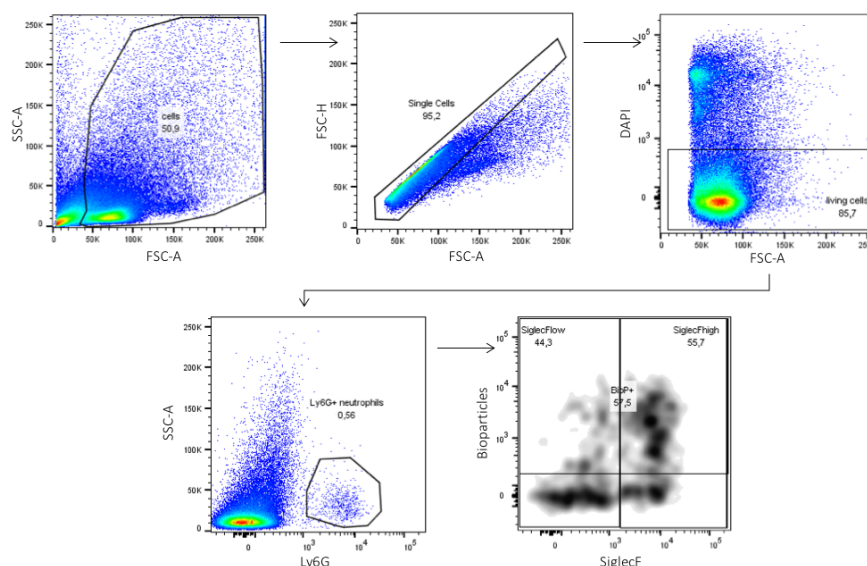


Figure 4.12 Gating strategy of neutrophils incubated with PHrodo™ Green *E. coli* BioParticles® Conjugate

Cells identified as SSC-A and FSC-A positive. Removal of doublets by gating single cells. Exclusion of dead cells by gating living cells as DAPI-. Gating neutrophils as Ly6G+. Defining the gate for BioParticle+/- neutrophils and distinguishing between SiglecF^{high} / low neutrophils.

In both experimental groups, neutrophils isolated from 3-day-old infarcted hearts showed higher proportions of SiglecF^{high} neutrophils compared to neutrophils isolated at day 1 after infarction, as seen in previous experiments (fig. 4.13 A).

Only $34.2 \pm 6.3\%$ of SiglecF^{low} neutrophils isolated at D3 after myocardial infarction showed phagocytosis of bioparticles, compared to $63.2 \pm 7.8\%$ of SiglecF^{high} expressing neutrophils, thus showing their greater ability to phagocytose E. coli derived bioparticles (P = 0.0002) (fig. 4.13 B).

Neutrophils isolated from 1-day-old infarcted hearts showed a similar ability to phagocytose as SiglecF^{high} neutrophils isolated from 3-day-old ischemic hearts ($55.4 \pm 6.3\%$ of the total neutrophils isolated at MI D1) (fig. 4.13 B).

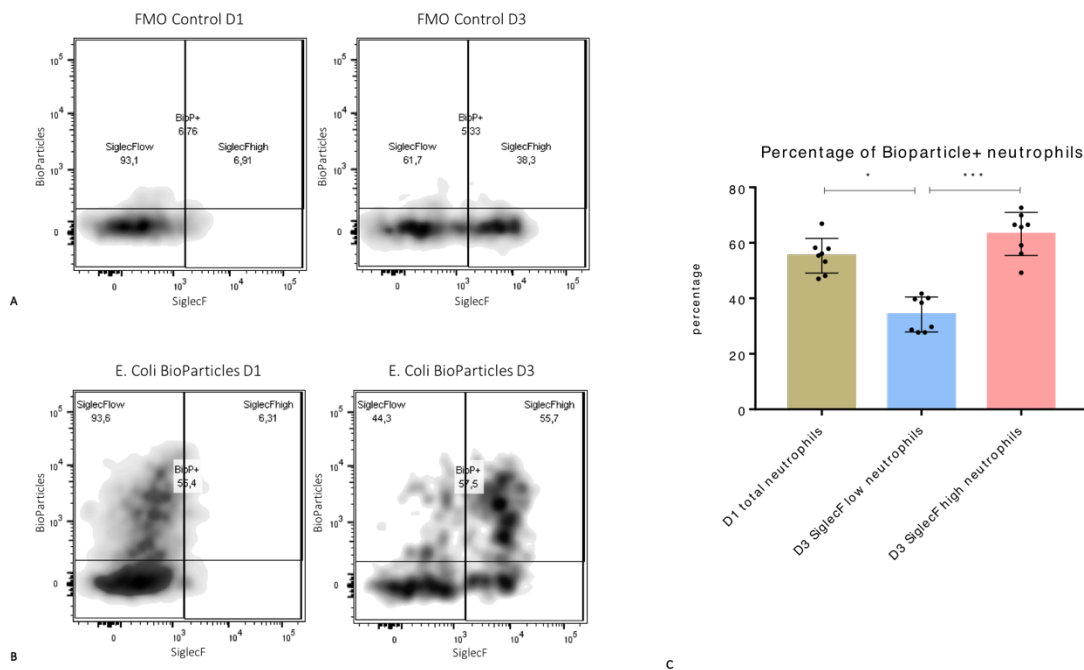


Figure 4.13 Phagocytosis of E. coli bioparticles in neutrophil subsets

A Representative example of FACS dot plots of FMO control groups in neutrophil subsets 1 and 3 days after myocardial infarction. Defining the gate for Bioparticle+ neutrophils in the FMO control group. Distinguishing between SiglecF^{high} / low neutrophils.

B Representative example of FACS dot plots of phagocytosis of E. coli bioparticles in neutrophil subsets 1 and 3 days after myocardial infarction. Distinguishing between SiglecF^{high} / low neutrophils.

C percentage of phagocytosis in different neutrophil subsets. *p < 0.05; ***p < 0.001

4.5.2. ROS production

Mice with myocardial infarction were sacrificed at either day 1 or day 3 after infarction. Processed heart cell suspensions were incubated with DHR123 (final concentration: 1/200) and divided into two experimental groups. One group was incubated for 30 minutes at 4°C to serve as a negative control. The second group was incubated for 30 minutes at 37°C. Neutrophils isolated from hearts 1 or 3 days after MI were gated as living, Ly6G+ cells. Neutrophils from 3-day-old infarcted hearts were furthermore distinguished between in terms of SiglecFhigh and SiglecFlow neutrophils (fig 4.14).

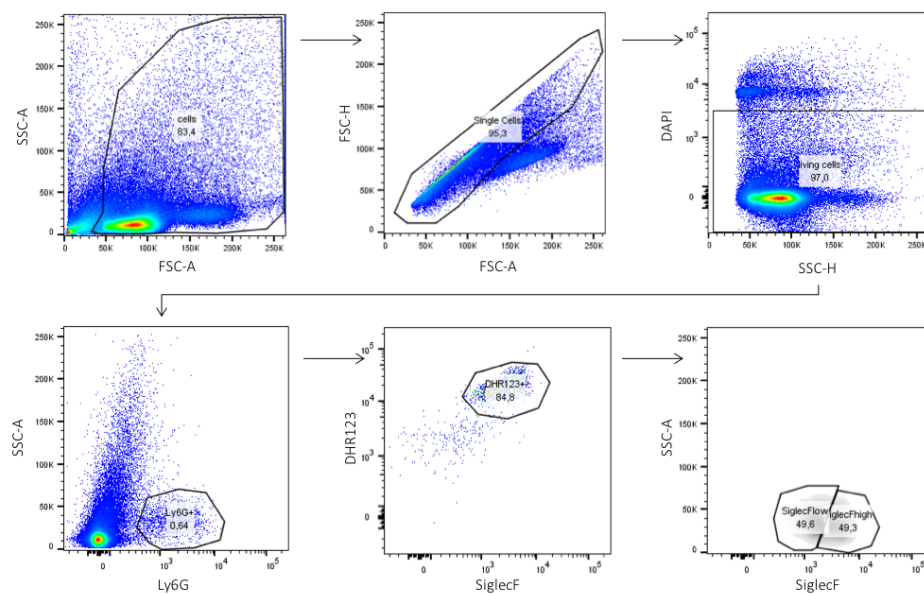


Figure 4.14 Gating strategy of neutrophils incubated with DHR123

Cells identified as SSC-A and FSC-A positive. Removal of doublets by gating single cells. Exclusion of dead cells by gating living cells as DAPI-. Gating neutrophils as Ly6G+. Defining the gate for DHR123+ neutrophils and distinguishing between SiglecFhigh / low neutrophils.

The geometric mean of light emitted from the ROS-dependent fluorescing derivates was compared. Greater production of reactive oxygen species results in higher fluorescence intensity, i.e. a higher geometric mean.

SiglecFhigh neutrophils isolated from 3-day-old infarcted hearts showed much higher ROS production rates (Geometric Mean FITC: 20364 ± 2218) than SiglecFlow neutrophils (Geometric Mean FITC: 14909 ± 1372), which indicates their greater capacity for ROS production ($P < 0.0001$).

Neutrophils isolated from 1-day-old infarcted hearts* showed a similar ROS production capacity (Geometric Mean FITC: 18311 ± 899) to SiglecFlow expressing neutrophils from 3-day-old ischemic hearts (fig.4.15).

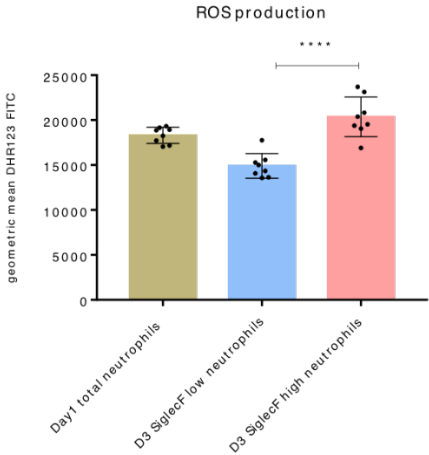


Figure 4.15 Reactive oxygen species (ROS) production in neutrophil subsets
Geometric mean of DHR123 fluorescence in different neutrophil subsets. **** p < 0.0001

4.6. Investigation of the time-dependent role and functional impact of neutrophil subpopulations—depletion experiments

In vivo depletion of neutrophils allows changes in neutrophil heterogeneity and their functional effect on cardiac repair to be investigated. Depending on their temporal appearance after the onset of ischemia, a timed depletion can help to better understand functional differences in these neutrophil subpopulations in the ischemic heart.

4.6.1. Neutrophils can be identified independently of Ly6G by detecting them via CXCR2

For a first in vivo depletion experiment involving neutrophils, a previously published protocol was followed using anti-Ly6G antibodies (25) binding themselves to the epitope 1A8, which is also commonly used to detect and identify neutrophils via flow cytometry.

As these depleting antibodies could also veil the epitope and thereby avoid revealing non-depleted neutrophils such as Ly6G⁺ (47) (fig.4.16), a new protocol was established to reliably detect neutrophils independently of Ly6G via flow cytometry.

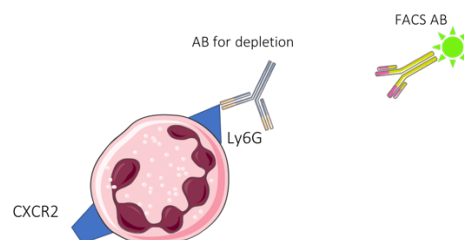


Figure 4.16 Schematic chart of depleting and FACS antibodies binding themselves to the epitope 1A8

CXCR2 served as an alternative marker for neutrophils. Previous experiments showed that enzymatic processing of the infarcted hearts had effects on the surface marker CXCR2 (not shown). Therefore, hearts were processed via mechanical digestion.

Neutrophils were isolated from control hearts as well as from 1-day-old ischemic hearts and processed via mechanical digestion for flow cytometry analysis. Neutrophils were gated as viable CD45⁺CD11b⁺CD64⁻CXCR2⁺ cells. CD64 served as an exclusion marker as it is only expressed by monocytes and macrophages but not neutrophils (fig 4.17).

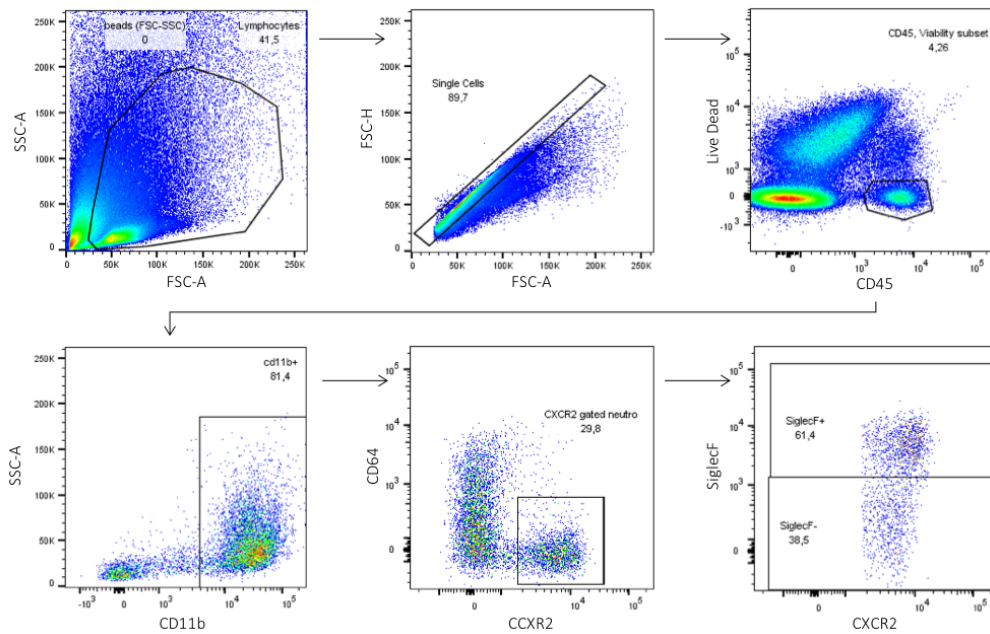


Figure 4.17 Gating strategy of cardiac neutrophils gated as CXCR2+ cells

Cells identified as SSC-A and FSC-A positive. Removal of doublets by gating single cells. Exclusion of dead cells by gating living cells as e780- and defining leucocytes as CD45+. Gating myeloid cells as CD11b+. Exclusion of monocytes / macrophages using CD64. Identification of neutrophils gated as CD64-CXCR2+ cells. Defining SiglecF^{high} and SiglecF^{low} CXCR2+ neutrophils.

To verify if these cells were truly neutrophils, the proportion of Ly6G⁺ neutrophils was calculated from this gated population. 98.4% of the CXCR2⁺ gated neutrophils were also Ly6G⁺, thus confirming them as neutrophils. To investigate if there could be leftover neutrophils that had not been detected via CXCR2, all leftover cells were gated reversely to screen them for Ly6G. Only 0.038% of these reversely gated CXCR2⁻ cells were Ly6G⁺, confirming that using the CD11b⁺CXCR2⁺ combination is a reliable method to identify neutrophils via flow cytometry independently of surface Ly6G expression (fig 4.18).

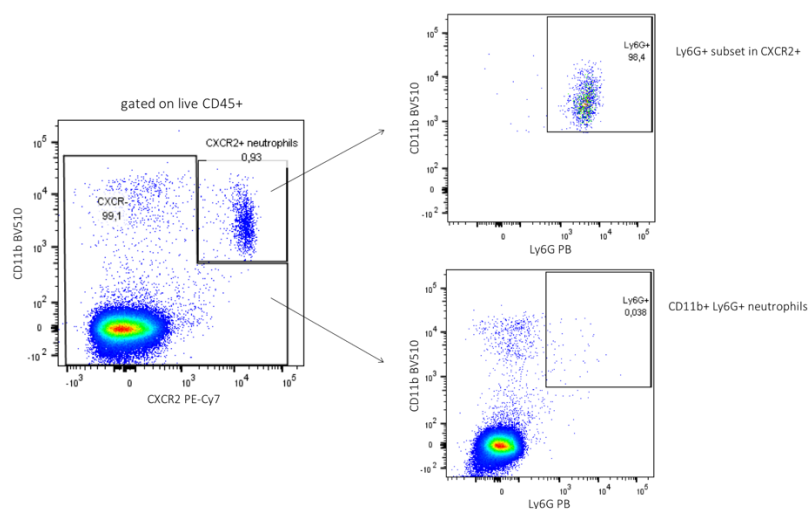


Figure 4.18 Neutrophils can be reliably identified independently of surface Ly6G expression
Neutrophils gated as CD45⁺CD11b⁺CXCR2⁺ cells

4.6.2. Anti-Ly6G treatment fails to achieve successful neutrophil depletion at day 3 post MI

In this first in vivo depletion experiment, an established protocol from Horckmans et al. was followed to obtain results directly comparable with previously published data (25). Time-dependent depletion of neutrophils was performed using the anti-Ly6G monoclonal antibody clone 1A8.

Mice were divided into four experimental groups, where the injection of anti-Ly6G started at different time points before and after myocardial infarction.

For one group, depletion started 1 day before myocardial infarction to achieve neutrophil depletion before the onset of cardiac ischemia. For the second group, depletion started 1 day after myocardial infarction to preferentially deplete SiglecFlow neutrophils that are mainly present at D1–2 after myocardial infarction. For the third group, depletion started 2 days after myocardial infarction to target SiglecFhigh neutrophils, which are mainly present at D3 after myocardial infarction. Another group did not receive any injection of anti-Ly6G antibodies and served as a negative control. Instead, they received the appropriate isotype control antibody. Myocardial infarction was performed on all the experimental groups on the same day.

All the experimental groups were sacrificed at day 3 after myocardial infarction and their organs were processed for flow cytometry analyses (fig. 4.19).

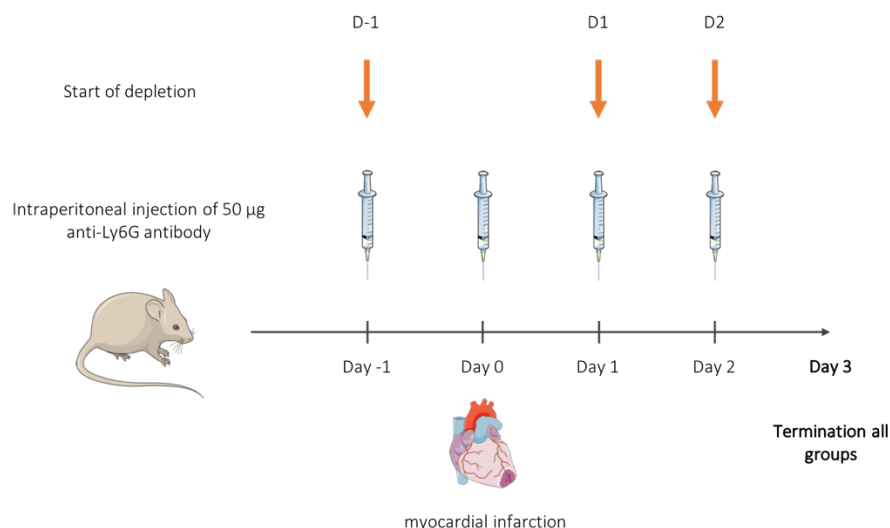


Figure 4.19 Experimental design of depletion experiment

4.6.2.1. Heart

For each sample, neutrophils were identified using two different gating strategies. For one gating strategy, neutrophils were identified as CD45+CD11b+CD64-Ly6G+ cells, which were then furthermore distinguished between in terms of SiglecFhigh and SiglecFlow neutrophils (fig. 4.1). For the second gating strategy, neutrophils were identified as CD45+CD11b+ CD64-CXCR2+ cells, which were then also furthermore distinguished between in terms of SiglecFhigh and SiglecFlow neutrophils (fig. 4.17) CD64 served as an exclusion marker as it is only expressed on monocytes and macrophages, but not on neutrophils.

As regards neutrophils gated as Ly6G+, all groups treated with Anti-Ly6G seemed to show successful depletion by having less than 1% leftover Ly6G+ neutrophils (fig. 4.20 A, C).

Surprisingly, when the results relating to when neutrophils were gated as CXCR2+ were compared, all experimental depletion groups still showed leftover CXCR2+ neutrophils (fig. 4.20 B, D).

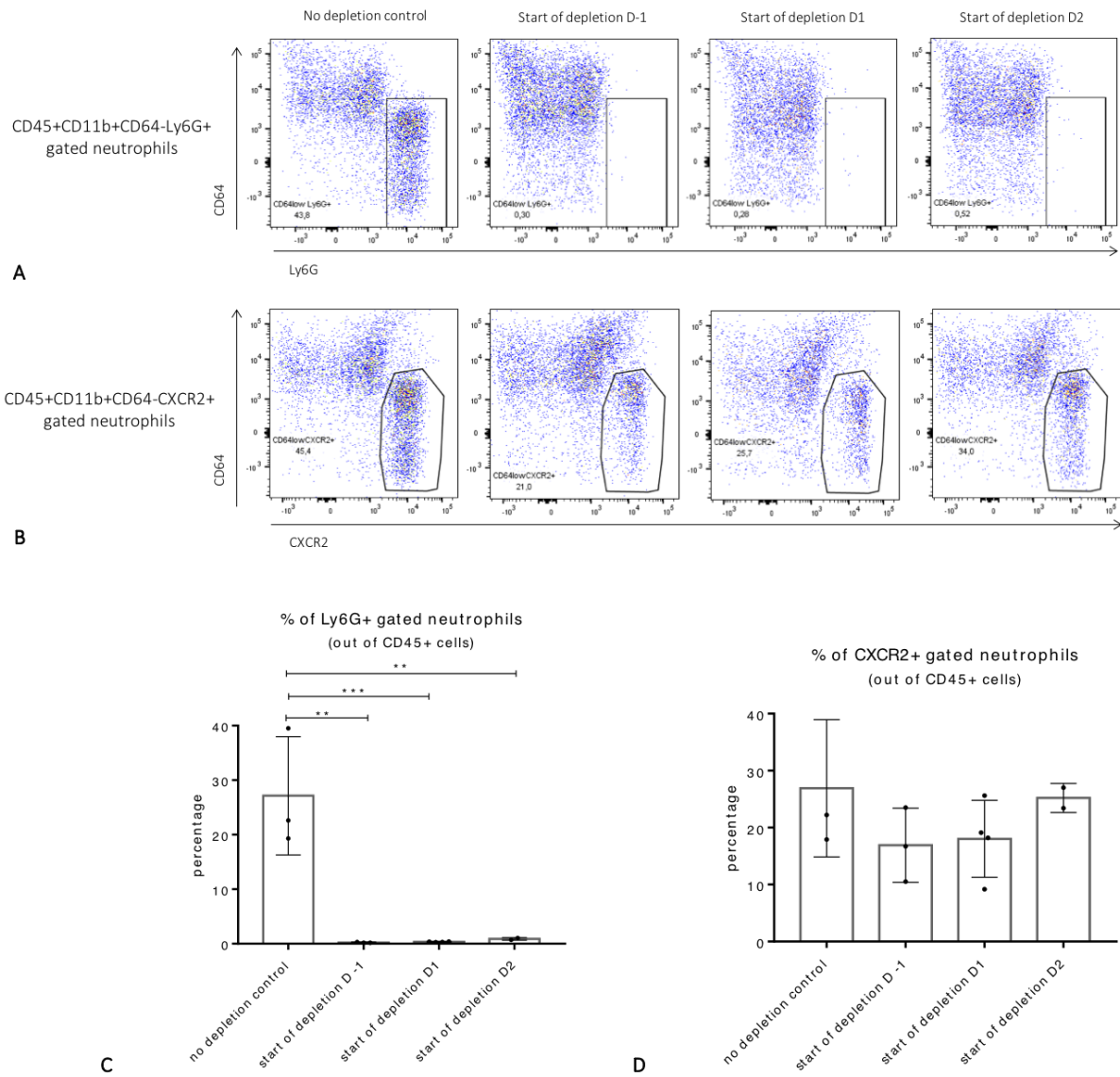


Figure 4.20 Anti-Ly6G treatment fails to achieve successful depletion of cardiac neutrophils 3 days after myocardial infarction

A Representative example of FACS dot plots of depleted cardiac neutrophils 3 days after myocardial infarction. Neutrophils pre-gated as CD45+CD11b+CD64- cells. Identification of neutrophils as CD64-Ly6G+ cells.

B Representative example of FACS dot plots of depleted cardiac neutrophils 3 days after myocardial infarction. Neutrophils pre-gated as CD45+CD11b+CD64- cells. Identification of neutrophils as CD64-CXCR2+ cells.

C Proportion of cardiac neutrophils in the experimental cohorts, gated as CD45+CD11b+CD64-Ly6G+ cells.

D Proportion of cardiac neutrophils in the experimental cohorts, gated as CD45+CD11b+CD64-CXCR2+ cells.

4.6.2.2. Shift of SiglecFhigh neutrophils in the cardiac tissue of depleted mice

As regards SiglecFhigh and SiglecFlow neutrophil proportions from CXCR2+ gated neutrophils, there were also clear differences regarding the proportions between the experimental groups. In all groups in which mice received neutrophil depleting anti-Ly6G antibodies, the proportions of SiglecFhigh expressing neutrophils were higher than in the non-depleted experimental control group (fig. 4.21).

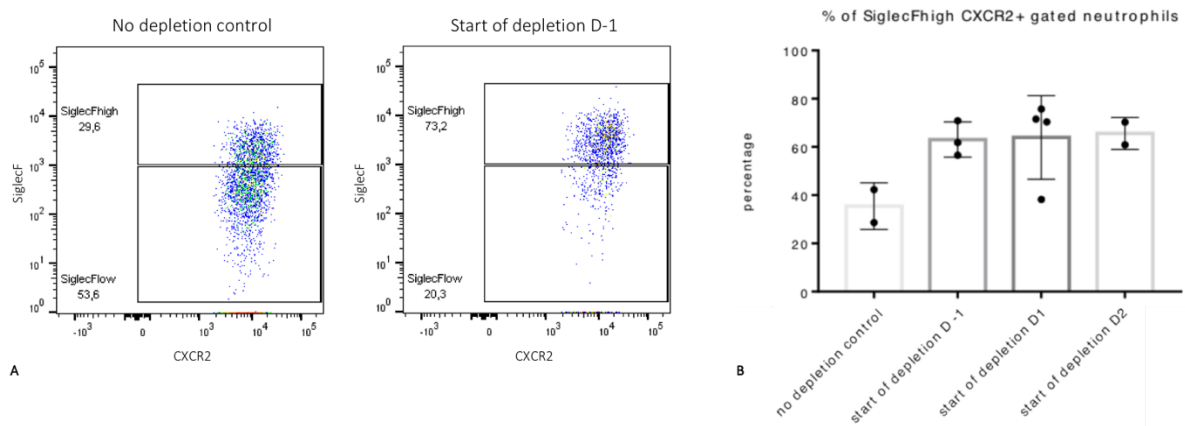


Figure 4.21 Shift of SiglecFhigh neutrophils in the cardiac tissue of depleted mice

A Representative example of FACS dot plots of CXCR2+SiglecFhigh neutrophils in the no depletion control group vs. depletion groups.

B Proportion of CXCR2+SiglecFhigh cardiac neutrophils in the different experimental cohorts.

4.6.2.3. Blood

For each sample, neutrophils were identified using the same gating strategies as described for the heart above.

As similarly observed in the heart, neutrophils gated as Ly6G+ seemed to be successfully depleted in the experimental depletion groups, constituting less than 1% of all CD45+ cells (fig 4.22 A, C). With regard to neutrophils gated as CXCR2+, there was a reduction of neutrophils in all the experimental depletion groups; however, leftover neutrophils were still detected (fig 4.22 B, D).

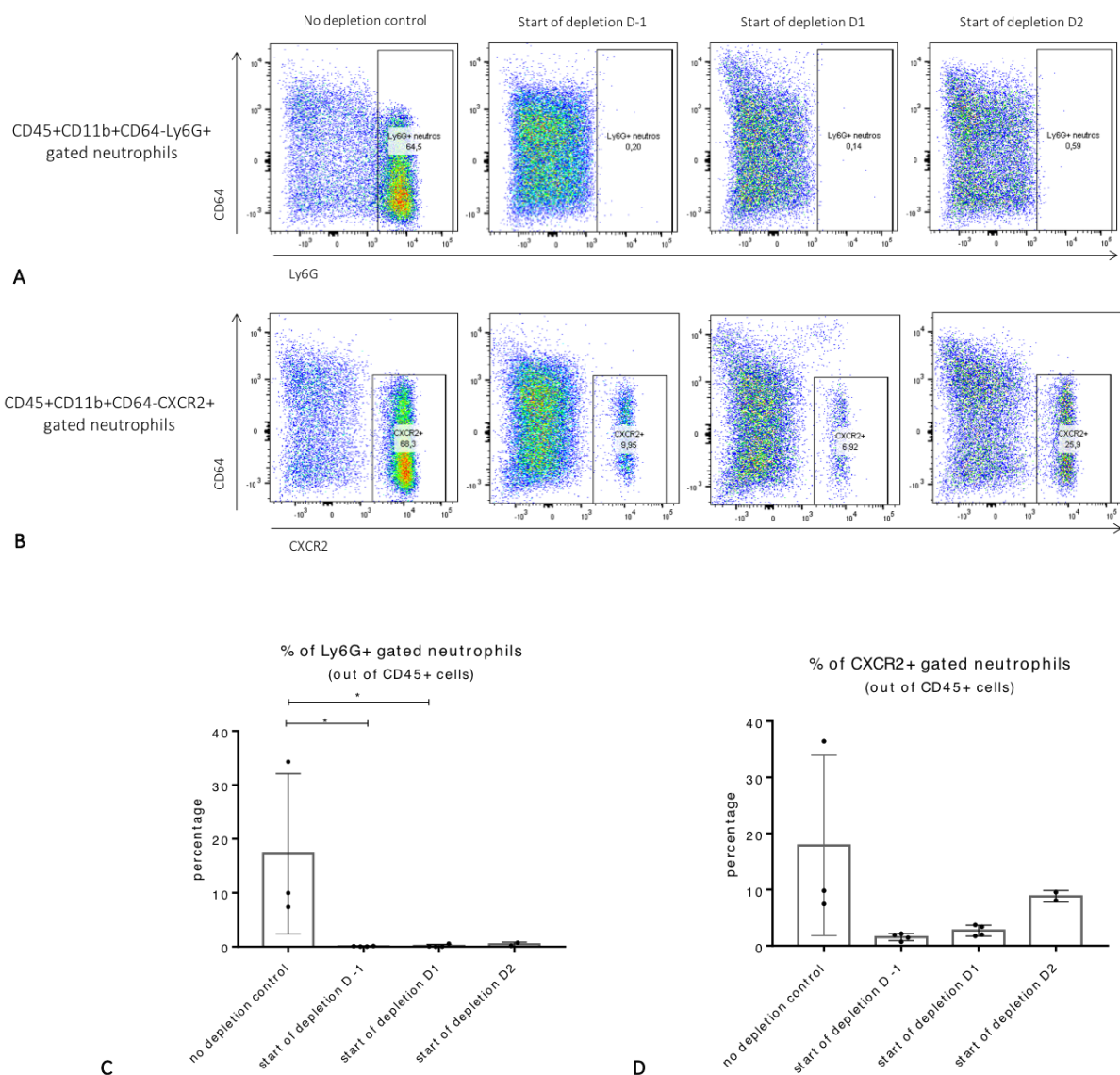


Figure 4.22 Anti-Ly6G treatment fails to achieve complete depletion of blood neutrophils 3 days after myocardial infarction

A Representative example of FACS dot plots of depleted blood neutrophils 3 days after myocardial infarction. Neutrophils pre-gated as CD45+CD11b+CD64- cells. Identification of neutrophils as CD64-Ly6G+ cells.

B Representative example of FACS dot plots of depleted blood neutrophils 3 days after myocardial infarction. Neutrophils pre-gated as CD45+CD11b+CD64- cells. Identification of neutrophils as CD64-CXCR2+ cells.

C Proportion of blood neutrophils in the experimental cohorts, gated as CD45+CD11b+CD64-Ly6G+ cells.

D Proportion of blood neutrophils in the experimental cohorts, gated as CD45+CD11b+CD64-CXCR2+ cells.

4.6.2.4. Bone marrow

Neutrophils were pre-gated as CD45+CD11b+CD115- and then furthermore identified as either Ly6G+ or CXCR2+, as described above. CD115 served as an exclusion marker for monocytes.

Neutrophils gated as Ly6G+ cells seemed to be successfully depleted in the experimental depletion groups, constituting less than 1% of CD45+ leucocytes (fig. 4.23 A, C).

As regards the proportions of neutrophils gated as CXCR2+, the experimental depletion groups showed a clear reduction with lower proportions but still no complete depletion of CXCR2+ neutrophils compared to the non-depleted control group (fig. 4.23 B, D).

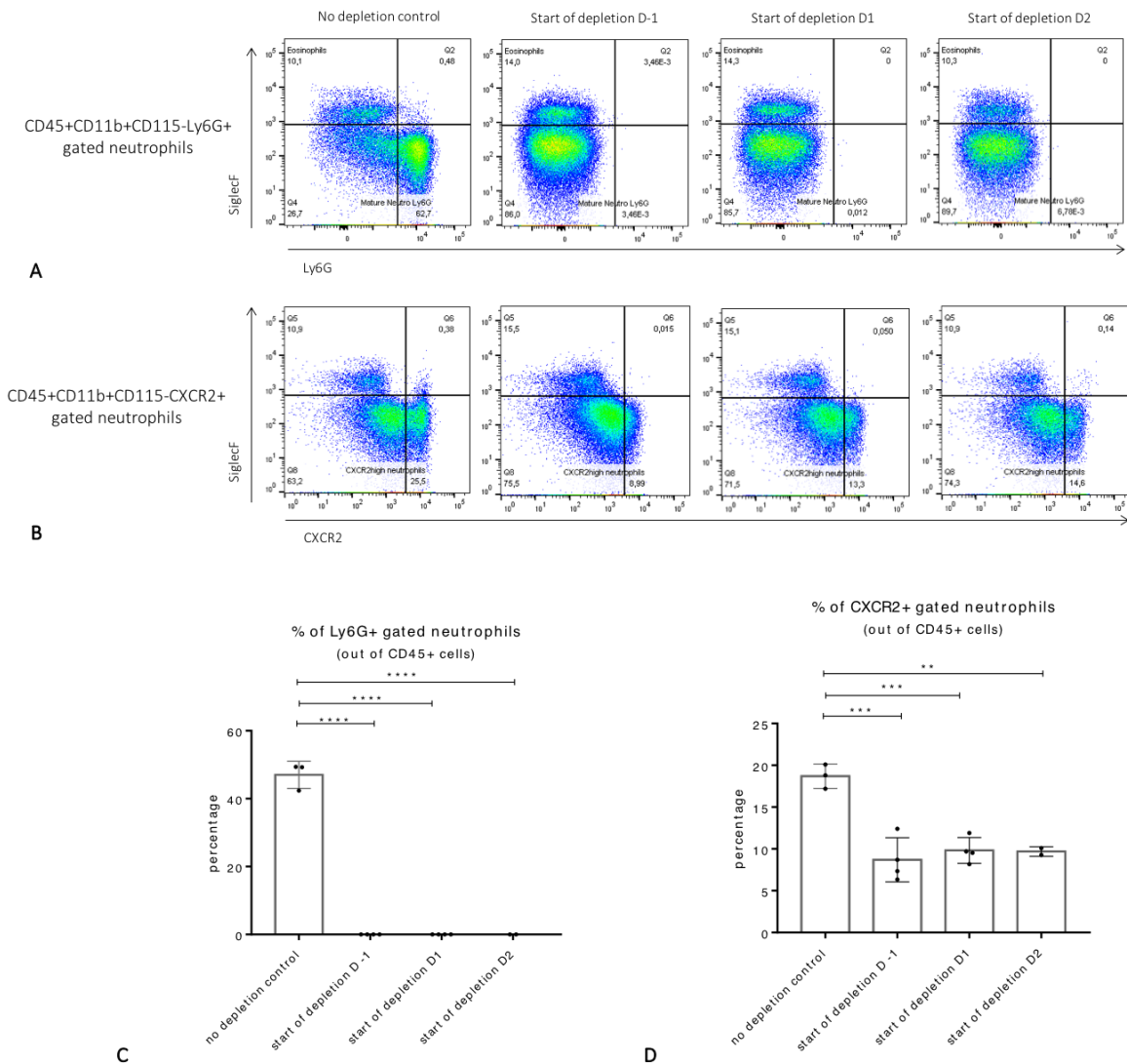


Figure 4.23 Anti-Ly6G treatment fails to achieve complete depletion of bone marrow neutrophils 3 days after myocardial infarction

A Representative example of FACS dot plots of depleted bone marrow neutrophils 3 days after myocardial infarction. Neutrophils pre-gated as CD45+CD11b+CD115- cells. Identification of neutrophils as CD115-Ly6G+ cells.

B Representative example of FACS dot plots of depleted bone marrow neutrophils 3 days after myocardial infarction. Neutrophils pre-gated as CD45+CD11b+CD115- cells. Identification of neutrophils as CD115-Ly6G+ cells.

C Proportion of bone marrow neutrophils in the experimental cohorts, gated as CD45+CD11b+CD115-Ly6G+ cells.

D Proportion of bone marrow neutrophils in the experimental cohorts, gated as CD45+CD11b+CD115-CXCR2+ cells.

4.6.2.5. Spleen

For each sample, neutrophils were identified using the same gating strategies as described for the heart above.

As similarly observed in the heart, blood and bone marrow, neutrophils identified as Ly6G+ cells seemed to be successfully depleted in the experimental depletion groups, representing less than 1% from CD45+ cells (fig. 4.24 A, C). Identifying neutrophils as CXCR2+, the depleted experimental groups showed lower proportions but still leftover non-depleted CXCR2+ neutrophils (fig 4.24 B, D).

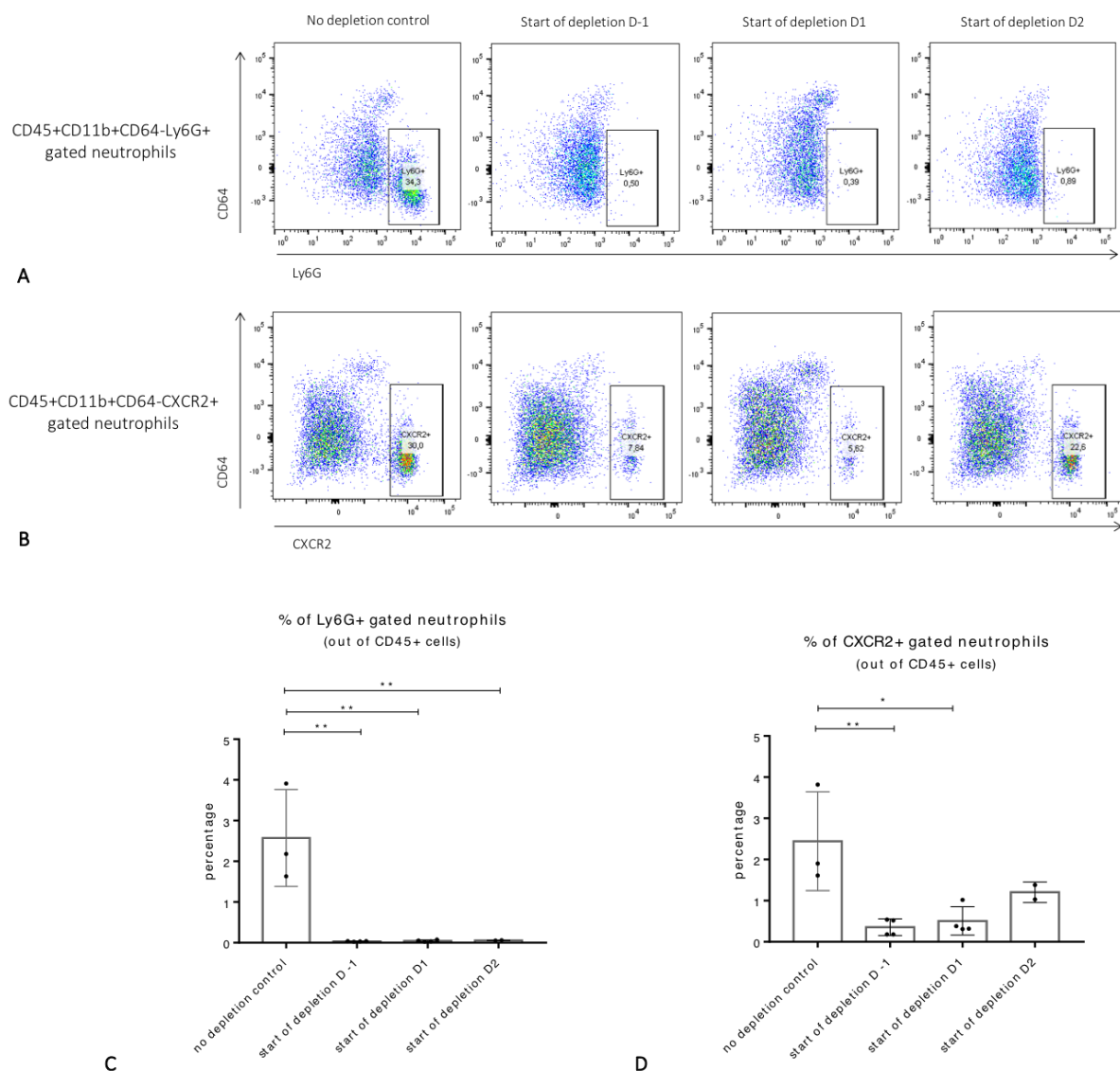


Figure 4.24 Anti-Ly6G treatment fails to achieve complete depletion of spleen neutrophils 3 days after myocardial infarction

A Representative example of FACS dot plots of depleted spleen neutrophils 3 days after myocardial infarction. Neutrophils pre-gated as CD45+CD11b+CD64- cells. Identification of neutrophils as CD64-Ly6G+ cells.

B Representative example of FACS dot plots of depleted spleen neutrophils 3 days after myocardial infarction. Neutrophils pre-gated as CD45+CD11b+CD64- cells. Identification of neutrophils as CD64-CXCR2+ cells.

C Proportion of spleen neutrophils in the experimental cohorts, gated as CD45+CD11b+CD64-Ly6G+ cells.

D Proportion of spleen neutrophils in the experimental cohorts, gated as CD45+CD11b+CD64-CXCR2+ cells.

To summarize, anti-Ly6G depletion of neutrophils failed to completely reduce neutrophil levels in the observed organs 3 days after myocardial infarction.

Especially in the heart, neutrophil levels did not show a significant decrease from the no depletion control group to the depletion groups. Instead, there was a shift towards a higher proportion of SiglecF^{high} neutrophils in the depletion groups.

Depletion of neutrophils seemed to be quite efficient in the blood as well as in the spleen, even though no complete depletion could be achieved.

In the bone marrow, partial depletion was observed.

4.6.3. Confirmation of inefficient anti-Ly6G depletion of neutrophils 1 and 3 days after myocardial infarction

To confirm the results from the previous *in vivo* depletion experiment, another similar experiment was performed with a higher number of mice, employing the same established protocol from Horckmans et al. (25) as in the previous depletion experiment.

The first depletion experiment was unable to show successful depletion of neutrophils at day 3 after myocardial infarction. To investigate whether these results could be explained by the higher production and release of young neutrophils due to emergency granulopoiesis after myocardial infarction, neutrophil depletion efficacy was also observed at day 1 after myocardial infarction.

Mice received a daily intraperitoneal injection of 50µg anti-Ly6G antibody clone 1A8 or the appropriate isotype control starting 1 day before the induction of myocardial infarction to consistently deplete neutrophils until the mice were sacrificed.

Organs from mice with 1 and 3-day-old infarcted hearts were processed and analyzed via flow cytometry. All analyses were performed the same day to create identical experimental conditions for all the experimental groups.

Neutrophils were identified using the same two different gating strategies as described above in the previous depletion experiment (fig. 4.1; fig. 4.17).

4.6.3.1. *Anti-Ly6G treatment fails to achieve complete neutrophil depletion at day 1 post-MI*

With regard to neutrophils isolated from 1-day-old ischemic hearts identified as CXCR2+, anti-Ly6G antibody depleted mice showed lower proportions of but still leftover cardiac neutrophils, representing $22.6 \pm 5.1\%$ of CD45+ cells compared to $59.4 \pm 6.7\%$ in the no depletion control group ($P = 0.09$) (fig. 4.25 A).

As in previous experiments, neutrophils isolated from 1-day-old infarcted hearts were SiglecFlow in both experimental groups (not shown).

As already seen at day 3 after myocardial infarction, blood neutrophils isolated from anti-Ly6G depleted mice showed a stronger reduction of neutrophil levels compared to no depletion controls. This reduction of neutrophils in the blood seemed to be more efficient than the reduction of neutrophils in the ischemic hearts 1 day after myocardial infarction.

The proportion of CXCR2+ blood neutrophils identified decreased from $26.3 \pm 11.1\%$ in the isotype control group to $3.6 \pm 2.4\%$ in the depletion group ($P = 0.05$) (fig. 4.25 B).

Depletion of neutrophils via the anti-Ly6G antibody did not show any considerable effect on neutrophil levels in the bone marrow at day 1 after myocardial infarction (fig. 4.25 C).

Anti-Ly6G depletion of neutrophils failed to achieve a significant reduction of neutrophils in the spleen 1 day after myocardial infarction. The experimental group treated with anti-Ly6G-antibodies showed lower proportions but still leftover non-depleted CXCR2+ neutrophils (fig. 4.25 D).

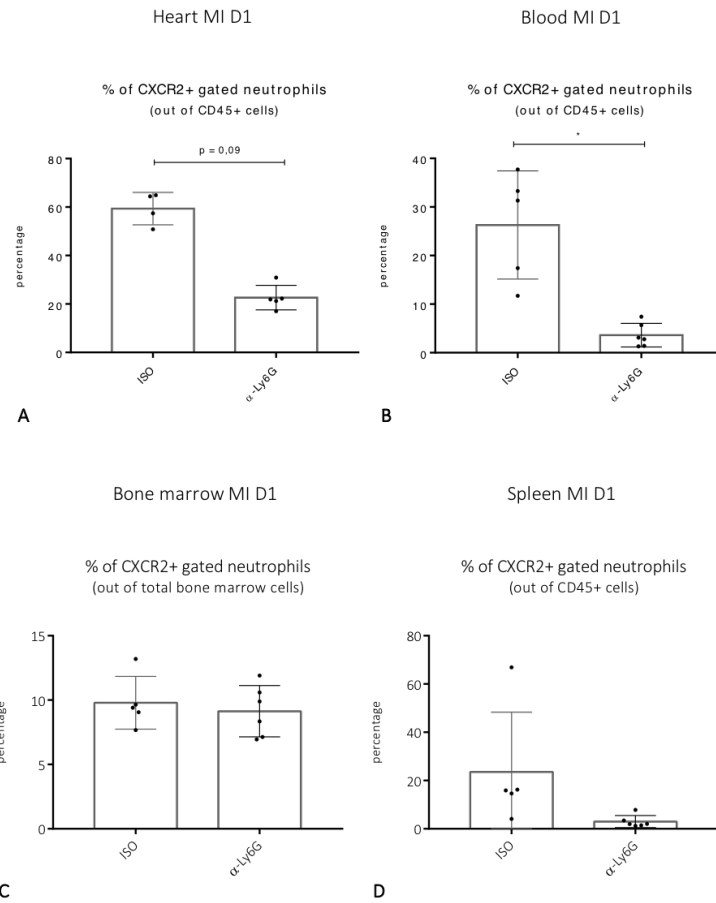


Figure 4.25 Anti-Ly6G treatment fails to achieve complete depletion of neutrophils 1 day after myocardial infarction
A Proportion of CD45+CD11b+CXCR2+ cardiac neutrophils 1 day after myocardial infarction (in % of total CD45+ cells).
B Proportion of CD45+CD11b+CXCR2+ blood neutrophils 1 day after myocardial infarction (in % of total CD45+ cells).
C Proportion of CD45+CD11b+CXCR2+ bone marrow neutrophils 1 day after myocardial infarction (in % of total CD45+ cells).
D Proportion of CD45+CD11b+CXCR2+ spleen neutrophils 1 day after myocardial infarction (in % of total CD45+ cells).
 ISO: Isotype control group. A-Ly6G: depletion group.

4.6.3.2. *Anti-Ly6G treatment fails to achieve complete neutrophil depletion at day 3 post-MI*

If we compare the results from processed organs 3 days after myocardial infarction with the previous experiment, the results are reproduced.

In the cardiac tissue of the experimental depletion group, which was treated with the anti-Ly6G antibody, no Ly6G+ gated neutrophils were detected, whereas abundant neutrophils identified as CXCR2+ were found, thus confirming the previous results from the first depletion experiment that identifying neutrophils as Ly6G+ overestimates depletion efficacy.

Depletion in the heart was rather inefficient, with CXCR2+ gated neutrophils representing $32.4 \pm 10.4\%$ of CD45+ cells in the isotype control group, compared to $15.5 \pm 6.3\%$ in the depletion group ($P = 0.051$) (fig. 4.26 A).

When we compared SiglecFhigh neutrophils in both experimental groups, there was again a shift towards higher SiglecFhigh neutrophil proportions in the anti-Ly6G depleted group, which represented $72.9 \pm 9.2\%$ of all neutrophils compared to $50.3 \pm 11.5\%$ of all neutrophils in the isotype control group ($P = 0.0027$) (fig. 4.26 B).

The proportion of SiglecFlow neutrophils decreased from $49.5 \pm 11.5\%$ in the isotype control group to $27.1 \pm 9.3\%$ in the anti-Ly6G depleted group ($P = 0.0027$) (fig. 4.26 B).

As regards blood neutrophils identified as Ly6G+, no cells were observed.

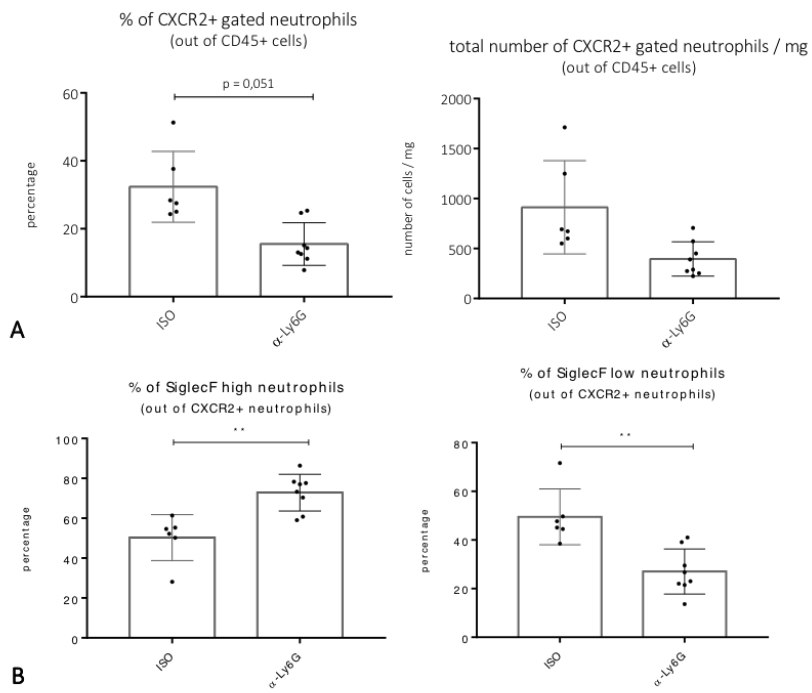
Blood neutrophils gated as CXCR2+ showed a strong reduction, decreasing from $12.6 \pm 8.6\%$ of CD45+ immune cells in the no depletion control group to $1.5 \pm 1.8\%$ in the depletion group ($P = 0.0132$) (fig. 4.26 C).

Bone Marrow

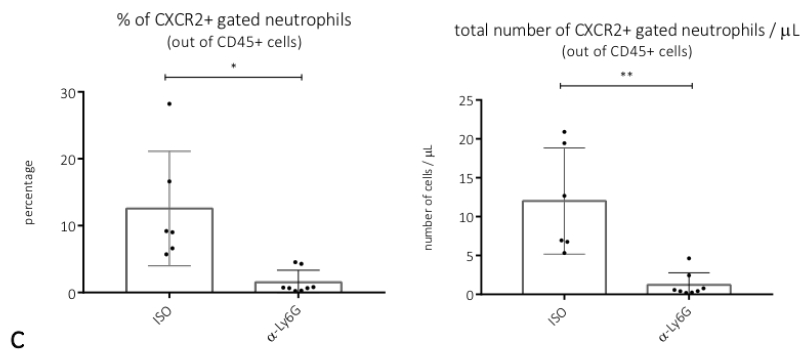
In this confirmation experiment, depletion of neutrophils via anti-Ly6G antibody only led to a partial reduction of neutrophil levels in the bone marrow 3 days after myocardial infarction, underlying the notion that anti-Ly6G antibodies fail to prevent infiltration of renewing bone marrow neutrophils infiltrating the infarcted heart (47) (fig. 4.26 D).

In the spleen, CXCR2+ neutrophils decreased from $4.9 \pm 2.5\%$ in the isotype control group to $0.8 \pm 0.7\%$ in the depletion group ($P = 0.0232$) (fig. 4.26 E).

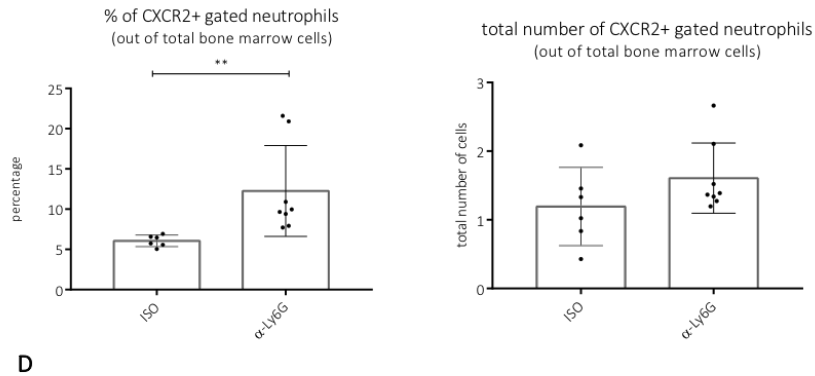
Heart MI D3



Blood MI D3

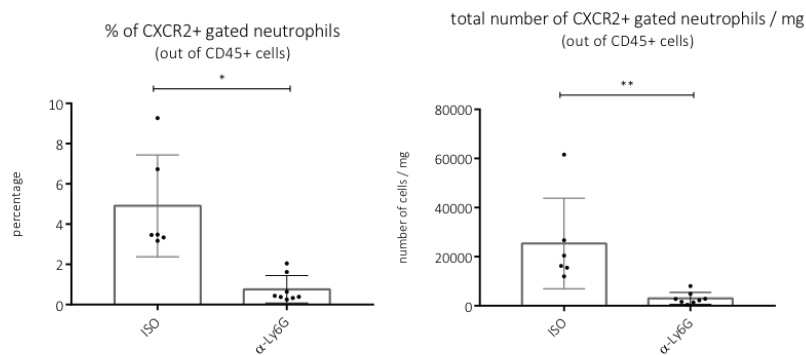


Bone marrow MI D3



D

Spleen MI D3



E

Figure 4.26 Validation depletion experiment

A Proportion (in % of total CD45+ cells) and total number of CD45+CD11b+CXCR2+ cardiac neutrophils 3 days after myocardial infarction.
B Proportion of CXCR2+SiglecF high and CXCR2+SiglecF low cardiac neutrophils (in % of total neutrophils) in experimental groups.
C Proportion (in % of total CD45+ cells) and total number of CD45+CD11b+CXCR2+ blood neutrophils 3 days after myocardial infarction.
D Proportion (in % of total CD45+ cells) and total number of CD45+CD11b+CXCR2+ bone marrow neutrophils 3 days after myocardial infarction.
E Proportion (in % of total CD45+ cells) and total number of CD45+CD11b+CXCR2+ spleen neutrophils 3 days after myocardial infarction.
 ISO: Isotype control group. A-Ly6G: depletion group.

Altogether, this in vivo experiment validated previous findings from the first depletion experiment. Anti-Ly6G treatment failed to achieve successful and efficient depletion of heart neutrophils at day 1 and day 3 after myocardial infarction. Levels of neutrophils in the bone marrow were not significantly affected by depletion 1 day after myocardial infarction but showed a partial reduction of levels 3 days after myocardial infarction, indicating that Anti-Ly6G antibodies fail to completely deplete renewing neutrophils in the bone marrow. Anti-Ly6G treatment rather efficiently reduced circulating blood neutrophils 1 day as well as 3 days after myocardial infarction, which may prevent infiltration of fresh SiglecFlow neutrophils into the infarcted heart and thereby lead to a local shift towards SiglecFhigh neutrophils in the heart at day 3 after myocardial infarction.

It is important to note that after treatment with anti-Ly6G antibodies for depletion, using Ly6G to gate neutrophils via flow cytometry, as done in previous studies, does not accurately measure real neutrophil levels but overestimates depletion.

5. Discussion

5.1. Time-dependent presence of different neutrophil states

Preliminary data from my working group revealed the time-dependent population of heterogeneous neutrophil clusters in the ischemic myocardium of mice. As regards their gene expression profiles, neutrophils isolated at later time points than 3 and 5 days after MI showed clear enrichment of *SiglecF* transcript levels compared to neutrophils at day 1 (43).

When we performed flow cytometry, these findings were confirmed on the protein level. Neutrophil infiltration peaked at day 1 after MI, showing lower counts at day 3 after MI (fig. 4.2). The main proportion of neutrophils isolated at day 3 after MI were SiglecF^{high} compared to only a small proportion at day 1 after MI, thus confirming results from preliminary data (fig. 4.4).

If we integrate data from previous scRNA-seq analyses of neutrophils with findings from flow cytometry results, SiglecF^{low} expressing neutrophils seem to represent young blood neutrophils by showing specific gene and surface marker expression patterns (*CD62Lhi*, *Sipi*, *Wfdc21*, *Retnlg*), whereas SiglecF^{high} expressing neutrophils shared some characteristics with circulating aged neutrophils (expression of specific transcripts such as *Icam1*, *Tnf*, *Cxcr4*, enrichment of ribosomal protein encoding genes, expression of surface markers such as ICAM1, CXCR4 or CD49d) (43).

5.2. Unique SiglecF^{high} state in the ischemic heart—a tissue restricted specification

The presence of SiglecF^{high} neutrophils was only found at day 3 but not at day 1 after MI. One possible explanation for this could be that SiglecF^{high} neutrophils represent a specific subset which is produced within the bone marrow during emergency granulopoiesis after the onset of cardiac ischemia, which is then released into the blood in order to infiltrate the ischemic myocardium and is therefore only present at later time points than 3 days after MI.

To verify this hypothesis, bone marrow, blood and spleen neutrophils were analyzed and compared in terms of their expression of SiglecF.

SiglecF^{high} neutrophils were only found in the heart at day 3 after MI, but not in the bone marrow, blood, or spleen 1 or 3 days after MI, which indicates that the presence of these neutrophils is tissue-specific for the ischemic heart. As evidence is rising that neutrophils have high plasticity potential, also in the setting of MI (25) (35), it is possible that neutrophils undergo a tissue-restricted specification. Further results of my working group supported this notion through differentiation trajectory inference by RNA-velocity (48) and pseudo-time ordering in Monocle (49), which indicates a specific aging process among neutrophils in ischemic cardiac tissue (43).

A more recent study also identified an SiglecF^{high} expressing neutrophil subtype which emerged late on in the setting of murine myocardial infarction. Findings regarding the origins of SiglecF^{high} expressing neutrophils suggested both some level of early fate specification as well as local activation within the heart (50).

SiglecF is a cell surface protein that has been described as inducing eosinophil apoptosis (46) (45). As the SiglecF expression of neutrophils arises at later time points after MI, when neutrophil counts are already getting lower, thus indicating resolution of their infiltration, it is possible that upregulation of SiglecF in neutrophils could be associated with increased neutrophil apoptosis. It could therefore be an active process that contributes to the resolution of inflammation after myocardial infarction.

5.3. Differences in functional capacities

To investigate whether neutrophil subpopulations found in the ischemic heart could exhibit functional differences, ROS production and phagocytosis activity of these subsets were investigated.

Compared to their SiglecF^{low} counterparts isolated at day 3, SiglecF^{high} neutrophils isolated 3 days after MI showed a greater ability to phagocytose as well as higher ROS production (fig. 4.13, fig. 4.14).

In a murine model of lung cancer, osteocalcin-expressing osteoblastic cells (Ocn⁺ cells) have been shown to supply lung tumors with a specific SiglecF^{high} neutrophil subset. Consistent with my results, these SiglecF^{high} neutrophils showed increased ROS production and promoted macrophage differentiation. Furthermore, they expressed genes associated with processes

that foster cancer, including angiogenesis, myeloid cell differentiation and recruitment, extracellular matrix remodeling, suppression of T cell responses, and tumor cell proliferation and growth (51).

In a murine model of MI, a population of SiglecF^{high} neutrophils that emerged late on was found in the ischemic heart. Compared to other neutrophil subsets, SiglecF^{high} neutrophils exhibited high levels of Myc-regulated genes as well as the activation of NFκB, which are associated with longevity. Functional enrichment analysis also revealed overexpression of genes involved in oxidative phosphorylation, which suggests that SiglecF^{high} neutrophils show increased ROS production (50).

Further results of my working group showed that cardiac SiglecF^{high} neutrophils also expressed high levels of ICAM1 (43), which can drive effector functions such as ROS production and phagocytosis (52).

Although these results underly the functional differences between SiglecF^{high} and SiglecF^{low} neutrophils, it remains unclear what role SiglecF^{high} neutrophils play within the ischemic heart. In a mouse model of MI, eosinophil depletion via anti-SiglecF treatment led to attenuated anti-inflammatory macrophage polarization, enhanced myocardial infarction, increased scar size, and deterioration of the myocardial structure and function (53). This could possibly indicate the beneficial effects of SiglecF^{high} expressing neutrophils in the setting of MI.

In a murine model of chronic kidney disease, Ryu et al. found a population of SiglecF^{high} neutrophils in the injured kidney. These SiglecF^{high} neutrophils were characterized by more frequent hyper-segmentation, higher expression of profibrotic inflammatory cytokines, and expression of collagen. Depletion of these SiglecF^{high} neutrophils reduced collagen deposition and disease progression (54). These findings suggest that profibrotic SiglecF^{high} neutrophils found in renal fibrosis could also be profibrotic in the ischemic heart.

5.4. Depletion of neutrophils via Anti-Ly6G-antibodies failed to fully deplete cardiac neutrophils but induced a shift towards more SiglecF^{high} neutrophils

SiglecF^{high} neutrophils were only found in the ischemic cardiac tissue at day 3 after MI, but not at earlier time points or other sites such as the bone marrow, blood, or spleen. The functional differences between the SiglecF^{high} neutrophils isolated at day 3 after MI were evidenced with

a greater ability to phagocytose as well as higher ROS production compared to their SiglecF^{low} counterparts.

Nevertheless, the functional consequences of the time-dependent heterogeneity of distinct neutrophil populations in the ischemic heart are not clear.

By performing antibody depletion of neutrophils *in vivo*, I tried to modulate neutrophil levels at different time points after MI in order to see changes in neutrophil subset presence in the ischemic heart.

With regard to ischemic cardiac tissue, all the results showed that depleting neutrophils through anti-Ly6G treatment failed to restrict the initial influx of neutrophils into the ischemic site, as neutrophils were still detected in the infarcted heart. If we look at neutrophil levels in the blood 1 and 3 days after MI, *in vivo* depletion induced a rather efficient reduction, which underlies the fact that the influx of neutrophils from the blood into the heart could not be completely prevented by *in vivo* depletion.

Instead, anti-Ly6G treatment in the experimental group led to a higher proportion of SiglecF^{high} neutrophils compared to the control groups, which supports the hypothesis that neutrophils shift locally towards a SiglecF^{high} state in the heart.

Neutrophil levels were not significantly affected in the bone marrow 1 and 3 days after MI, which is consistent with the results from Boivin et al., where anti-Ly6G depletion did not deplete neutrophils within the bone marrow (47).

Altogether, these results show that anti-Ly6G treatment *in vivo* not only leads to functional changes by reducing neutrophil levels (25) but can also cause phenotypic changes in neutrophil populations (47).

To better target neutrophil depletion *in vivo*, more efficient or different anti-neutrophil strategies are needed.

Boivin et al. recently described that after anti-Ly6G treatment, neutrophils are freshly generated in the bone marrow and exhibit a lower expression of Ly6G, thereby developing the ability to escape anti-Ly6G treatment. To obtain durable and controlled depletion of neutrophils, a double antibody-based depletion strategy has been proposed (47).

Another way to achieve successful neutrophil depletion are neutrophil deficient mouse models. By crossing MRP8-Cre mice with ROSA-iDTR^{K1} mice, PMN^{DTR} mice can be generated, in which neutrophils can be depleted by treatment with a diphtheria toxin (55).

Also, there are mouse models with constitutive neutropenia, such as G-CSFR^{-/-} mice and

CXCR2^{-/-} mice. However, mice with constitutive neutropenia have a higher risk of infections, and each model has its limitations, as is reviewed by Stackowicz et al. (56).

As regards our main neutrophil subsets found at day 3 after MI, SiglecF^{high} neutrophils with higher ROS production and a greater ability to phagocytose and their SiglecF^{low} counterparts, it would be interesting to preferentially deplete these neutrophil subtypes.

A recent study showed that anti-SiglecF treatment led to attenuated anti-inflammatory macrophage polarization, enhanced myocardial inflammation, increased scar size, and deterioration of the myocardial structure and function (53), which possibly indicates the beneficial effects of SiglecF^{high} neutrophils in the ischemic heart. Nevertheless, this anti-SiglecF treatment aimed to target eosinophils, thus a highly nuanced evaluation of the effects of anti-SiglecF treatment on eosinophils vs. SiglecF^{high} neutrophils in the setting of MI needs to be carried out.

Still, a full understanding of the dynamics and plasticity of these immune cells is lacking. Also, the effects of immune cell to immune cell interaction during the inflammatory response in the ischemic heart are unclear.

Despite the fact that neutrophils have long been considered detrimental in the setting of MI, there is growing evidence that neutrophils also play a positive, pro-reparative role. It is therefore necessary to take these protective functions into consideration when looking for depletion models. Anti-inflammatory strategies, which could be used to treat the detrimental effects of an inflammatory response after MI, should preferentially target the pro-inflammatory, detrimental effects of neutrophils, while maintaining or even supporting the anti-inflammatory, protective functions of neutrophils.

5.5. SiglecF^{high} neutrophils can also be found at different pathogenic sites

The SiglecF^{high} state of neutrophils was only found in the ischemic heart 3 days after myocardial infarction and showed differences in functions than phagocytosis or ROS production. To evaluate whether SiglecF^{high} neutrophils could also be observed in a more chronic cardiovascular disease context, my working group analyzed scRNAseq data from cells isolated from atherosclerotic aortas of low density lipoprotein receptor deficient (*Ldlr*^{-/-}) mice or control vessels of wild type mice. While no SiglecF^{high} neutrophils were found in the control

vessels, they were present in atherosclerotic aortas and aortic sinuses, which demonstrates that this specific neutrophil subset is also present in chronic cardiovascular diseases such as atherosclerosis (43).

In a mouse model of lung adenocarcinoma, a specific subset of neutrophils that infiltrate tumors was found, which was defined by their substantial expression of SiglecF. These SiglecF^{high} neutrophils expressed genes associated with processes that foster tumors, such as angiogenesis, myeloid cell differentiation and recruitment, extracellular matrix remodeling, suppression of T cell responses, and tumor cell proliferation and growth. Furthermore, these SiglecF^{high} neutrophils had increased ROS production, promoted macrophage differentiation, and boosted tumor progression *in vivo* (51).

Recently, Ryu et al. investigated the role of neutrophils in a mouse model of chronic kidney disease. Their results showed that kidney damage was associated with large amounts of a specific subset of SiglecF^{high} neutrophils. These SiglecF^{high} neutrophils promoted renal fibrosis by producing profibrotic cytokines as well as secreting collagen-1 by themselves. In contrast, their depletion reduced collagen deposition and disease progression (54).

More recently, Zilionis et al. compared myeloid cells that infiltrate tumors in human non-small cell lung cancer and in mouse lung adenocarcinoma to establish similarities and discrepancies between the two species. They identified three conserved modules of neutrophil gene expression within mouse and human neutrophils (57). As well as described before, they also found SiglecF^{high} neutrophils accumulated in tumor tissue and showed more pro-tumor functions than SiglecF^{low} neutrophils (51, 57). These findings indicate the possibility that specific neutrophil subsets found in the ischemic heart or other pathogenic sites could also be found in humans.

It is necessary to acquire more insight into distinct neutrophil states between mice and humans and especially into specific neutrophil states within the murine and ischemic heart to estimate the possible relevance of these subsets in an inflammatory response after myocardial infarction.

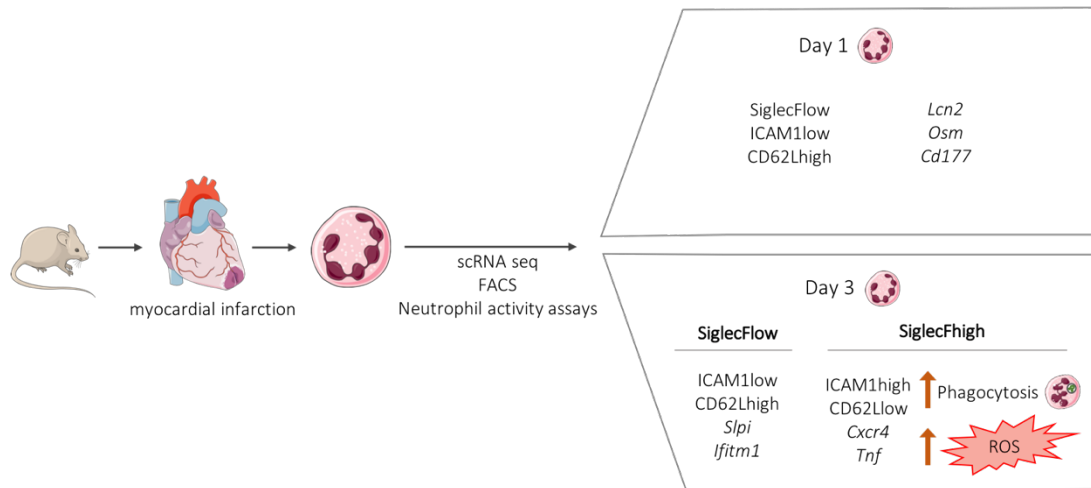


Figure 5.1 Graphical abstract

In a mouse model of myocardial infarction, the time-dependent presence of different neutrophil states in the ischemic heart was shown. These neutrophil states showed differences regarding their gene expression pattern, protein profile, and functional capacities. The majority of neutrophils isolated at day 3 after MI showed a high expression of SiglecF. This state was preserved in the ischemic heart and could not be detected at different time points or in other organs. These SiglecFhigh neutrophils showed a greater ability to phagocytose and higher ROS production than their SiglecFlow counterparts.

References

1. Puhl S-L, Steffens S. Neutrophils in Post-myocardial Infarction Inflammation: Damage vs. Resolution? *Front Cardiovasc Med.* 2019;6:25-.
2. Prabhu SD, Frangogiannis NG. The Biological Basis for Cardiac Repair After Myocardial Infarction: From Inflammation to Fibrosis. *Circulation research.* 2016;119(1):91-112.
3. Zlatanova I, Pinto C, Silvestre JS. Immune Modulation of Cardiac Repair and Regeneration: The Art of Mending Broken Hearts. *Front Cardiovasc Med.* 2016;3:40.
4. Peiseler M, Kubes P. More friend than foe: the emerging role of neutrophils in tissue repair. *The Journal of Clinical Investigation.* 2019;129(7):2629-39.
5. Shinagawa H, Frantz S. Cellular Immunity and Cardiac Remodeling After Myocardial Infarction: Role of Neutrophils, Monocytes, and Macrophages. *Current Heart Failure Reports.* 2015;12(3):247-54.
6. Ma Y, Yabluchanskiy A, Lindsey ML. Neutrophil roles in left ventricular remodeling following myocardial infarction. *Fibrogenesis Tissue Repair.* 2013;6(1):11.
7. Daseke MJ, 2nd, Chalise U, Becirovic-Agic M, Salomon JD, Cook LM, Case AJ, et al. Neutrophil signaling during myocardial infarction wound repair. *Cell Signal.* 2021;77:109816.
8. Ma Y. Role of Neutrophils in Cardiac Injury and Repair Following Myocardial Infarction. *Cells.* 2021;10(7):1676.
9. Phillipson M, Kubes P. The Healing Power of Neutrophils. *Trends Immunol.* 2019;40(7):635-47.
10. Liew PX, Kubes P. The Neutrophil's Role During Health and Disease. *Physiol Rev.* 2019;99(2):1223-48.
11. Jolly SR, Kane WJ, Hook BG, Abrams GD, Kunkel SL, Lucchesi BR. Reduction of myocardial infarct size by neutrophil depletion: effect of duration of occlusion. *Am Heart J.* 1986;112(4):682-90.
12. Dogan I, Karaman K, Sonmez B, Celik S, Turker O. Relationship between serum neutrophil count and infarct size in patients with acute myocardial infarction. *Nucl Med Commun.* 2009;30(10):797-801.
13. Askari AT, Brennan ML, Zhou X, Drinko J, Morehead A, Thomas JD, et al. Myeloperoxidase and plasminogen activator inhibitor 1 play a central role in ventricular remodeling after myocardial infarction. *J Exp Med.* 2003;197(5):615-24.
14. Vasilyev N, Williams T, Brennan ML, Unzek S, Zhou X, Heinecke JW, et al. Myeloperoxidase-generated oxidants modulate left ventricular remodeling but not infarct size after myocardial infarction. *Circulation.* 2005;112(18):2812-20.
15. Bidouard JP, Duval N, Kapui Z, Herbert JM, O'Connor SE, Janiak P. SSR69071, an elastase inhibitor, reduces myocardial infarct size following ischemia-reperfusion injury. *Eur J Pharmacol.* 2003;461(1):49-52.
16. van den Borne SW, Cleutjens JP, Hanemaaijer R, Creemers EE, Smits JF, Daemen MJ, et al. Increased matrix metalloproteinase-8 and -9 activity in patients with infarct rupture after myocardial infarction. *Cardiovasc Pathol.* 2009;18(1):37-43.
17. Ducharme A, Frantz S, Aikawa M, Rabkin E, Lindsey M, Rohde LE, et al. Targeted deletion of matrix metalloproteinase-9 attenuates left ventricular enlargement and collagen accumulation after experimental myocardial infarction. *J Clin Invest.* 2000;106(1):55-62.
18. Papayannopoulos V. Neutrophil extracellular traps in immunity and disease. *Nat Rev Immunol.* 2018;18(2):134-47.
19. Liu J, Yang D, Wang X, Zhu Z, Wang T, Ma A, et al. Neutrophil extracellular traps and dsDNA predict outcomes among patients with ST-elevation myocardial infarction. *Sci Rep.* 2019;9(1):11599.

20. Helseth R, Shetelig C, Andersen GO, Langseth MS, Limalanathan S, Opstad TB, et al. Neutrophil Extracellular Trap Components Associate with Infarct Size, Ventricular Function, and Clinical Outcome in STEMI. *Mediators Inflamm.* 2019;2019:7816491.
21. Grune J, Lewis AJM, Yamazoe M, Hulsmans M, Rohde D, Xiao L, et al. Neutrophils incite and macrophages avert electrical storm after myocardial infarction. *Nat Cardiovasc Res.* 2022;1(7):649-64.
22. Frangogiannis NG. Regulation of the inflammatory response in cardiac repair. *Circulation research.* 2012;110(1):159-73.
23. Soehnlein O, Lindbom L. Phagocyte partnership during the onset and resolution of inflammation. *Nat Rev Immunol.* 2010;10(6):427-39.
24. Lindsey ML, Jung M, Yabluchanskiy A, Cannon PL, Iyer RP, Flynn ER, et al. Exogenous CXCL4 infusion inhibits macrophage phagocytosis by limiting CD36 signalling to enhance post-myocardial infarction cardiac dilation and mortality. *Cardiovasc Res.* 2019;115(2):395-408.
25. Horckmans M, Ring L, Duchene J, Santovito D, Schloss MJ, Drechsler M, et al. Neutrophils orchestrate post-myocardial infarction healing by polarizing macrophages towards a reparative phenotype. *European Heart Journal.* 2016;38(3):187-97.
26. Ma Y, Mouton AJ, Lindsey ML. Cardiac macrophage biology in the steady-state heart, the aging heart, and following myocardial infarction. *Transl Res.* 2018;191:15-28.
27. Taichman NS, Young S, Cruchley AT, Taylor P, Paleolog E. Human neutrophils secrete vascular endothelial growth factor. *J Leukoc Biol.* 1997;62(3):397-400.
28. Christoffersson G, Vagesjo E, Vandooren J, Liden M, Massena S, Reinert RB, et al. VEGF-A recruits a proangiogenic MMP-9-delivering neutrophil subset that induces angiogenesis in transplanted hypoxic tissue. *Blood.* 2012;120(23):4653-62.
29. Massena S, Christoffersson G, Vagesjo E, Seignez C, Gustafsson K, Binet F, et al. Identification and characterization of VEGF-A-responsive neutrophils expressing CD49d, VEGFR1, and CXCR4 in mice and humans. *Blood.* 2015;126(17):2016-26.
30. Silvestre-Roig C, Hidalgo A, Soehnlein O. Neutrophil heterogeneity: implications for homeostasis and pathogenesis. *Blood.* 2016;127(18):2173-81.
31. Ng LG, Ostuni R, Hidalgo A. Heterogeneity of neutrophils. *Nature Reviews Immunology.* 2019;19(4):255-65.
32. Silvestre-Roig C, Fridlender ZG, Glogauer M, Scapini P. Neutrophil Diversity in Health and Disease. *Trends in Immunology.*
33. Uhl B, Vadlau Y, Zuchtriegel G, Nekolla K, Sharaf K, Gaertner F, et al. Aged neutrophils contribute to the first line of defense in the acute inflammatory response. *Blood.* 2016;128(19):2327-37.
34. Fridlender ZG, Sun J, Kim S, Kapoor V, Cheng G, Ling L, et al. Polarization of tumor-associated neutrophil phenotype by TGF-beta: "N1" versus "N2" TAN. *Cancer Cell.* 2009;16(3):183-94.
35. Ma Y, Yabluchanskiy A, Iyer RP, Cannon PL, Flynn ER, Jung M, et al. Temporal neutrophil polarization following myocardial infarction. *Cardiovascular Research.* 2016;110(1):51-61.
36. Yan X, Anzai A, Katsumata Y, Matsushashi T, Ito K, Endo J, et al. Temporal dynamics of cardiac immune cell accumulation following acute myocardial infarction. *J Mol Cell Cardiol.* 2013;62:24-35.
37. Daseke MJ, 2nd, Tenkorang-Impraim MAA, Ma Y, Chalise U, Konfrst SR, Garrett MR, et al. Exogenous IL-4 shuts off pro-inflammation in neutrophils while stimulating anti-inflammation in macrophages to induce neutrophil phagocytosis following myocardial infarction. *J Mol Cell Cardiol.* 2020;145:112-21.

38. Daseke MJ, 2nd, Valerio FM, Kalusche WJ, Ma Y, DeLeon-Pennell KY, Lindsey ML. Neutrophil proteome shifts over the myocardial infarction time continuum. *Basic Res Cardiol*. 2019;114(5):37-.
39. Dick SA, Macklin JA, Nejat S, Momen A, Clemente-Casares X, Althagafi MG, et al. Self-renewing resident cardiac macrophages limit adverse remodeling following myocardial infarction. *Nat Immunol*. 2019;20(1):29-39.
40. Peterson VM, Zhang KX, Kumar N, Wong J, Li L, Wilson DC, et al. Multiplexed quantification of proteins and transcripts in single cells. *Nat Biotechnol*. 2017;35(10):936-9.
41. Stoeckius M, Hafemeister C, Stephenson W, Houck-Loomis B, Chattopadhyay PK, Swerdlow H, et al. Simultaneous epitope and transcriptome measurement in single cells. *Nat Methods*. 2017;14(9):865-8.
42. Stoeckius M, Zheng S, Houck-Loomis B, Hao S, Yeung BZ, Mauck WM, 3rd, et al. Cell Hashing with barcoded antibodies enables multiplexing and doublet detection for single cell genomics. *Genome Biol*. 2018;19(1):224.
43. Vafadarnejad E, Rizzo G, Krampert L, Arampatzi P, Arias-Loza AP, Nazzal Y, et al. Dynamics of Cardiac Neutrophil Diversity in Murine Myocardial Infarction. *Circulation research*. 2020;127(9):e232-e49.
44. Heib T, Gross C, Muller ML, Stegner D, Pleines I. Isolation of murine bone marrow by centrifugation or flushing for the analysis of hematopoietic cells - a comparative study. *Platelets*. 2021;32(5):601-7.
45. Kiwamoto T, Katoh T, Evans CM, Janssen WJ, Brummet ME, Hudson SA, et al. Endogenous airway mucins carry glycans that bind Siglec-F and induce eosinophil apoptosis. *J Allergy Clin Immunol*. 2015;135(5):1329-40.e9.
46. Mao H, Kano G, Hudson SA, Brummet M, Zimmermann N, Zhu Z, et al. Mechanisms of Siglec-F-induced eosinophil apoptosis: a role for caspases but not for SHP-1, Src kinases, NADPH oxidase or reactive oxygen. *PLoS One*. 2013;8(6):e68143-e.
47. Boivin G, Faget J, Ancey P-B, Gkasti A, Mussard J, Engblom C, et al. Durable and controlled depletion of neutrophils in mice. *Nat Commun*. 2020;11(1):2762.
48. La Manno G, Soldatov R, Zeisel A, Braun E, Hochgerner H, Petukhov V, et al. RNA velocity of single cells. *Nature*. 2018;560(7719):494-8.
49. Trapnell C, Cacchiarelli D, Grimsby J, Pokharel P, Li S, Morse M, et al. The dynamics and regulators of cell fate decisions are revealed by pseudotemporal ordering of single cells. *Nat Biotechnol*. 2014;32(4):381-6.
50. Calcagno DM, Zhang C, Toomu A, Huang K, Ninh VK, Miyamoto S, et al. SiglecF(HI) Marks Late-Stage Neutrophils of the Infarcted Heart: A Single-Cell Transcriptomic Analysis of Neutrophil Diversification. *J Am Heart Assoc*. 2021;10(4):e019019.
51. Engblom C, Pfirschke C, Zilionis R, Da Silva Martins J, Bos SA, Courties G, et al. Osteoblasts remotely supply lung tumors with cancer-promoting SiglecF(high) neutrophils. *Science*. 2017;358(6367):eaal5081.
52. Woodfin A, Beyrau M, Voisin M-B, Ma B, Whiteford JR, Hordijk PL, et al. ICAM-1-expressing neutrophils exhibit enhanced effector functions in murine models of endotoxemia. *Blood*. 2016;127(7):898-907.
53. Toor IS, Ruckerl D, Mair I, Ainsworth R, Meloni M, Spiroski AM, et al. Eosinophil Deficiency Promotes Aberrant Repair and Adverse Remodeling Following Acute Myocardial Infarction. *JACC Basic Transl Sci*. 2020;5(7):665-81.
54. Ryu S, Shin JW, Kwon S, Lee J, Kim YC, Bae YS, et al. Siglec-F-expressing neutrophils are essential for creating a profibrotic microenvironment in renal fibrosis. *J Clin Invest*. 2022;132(12).

55. Reber LL, Gillis CM, Starkl P, Jonsson F, Sibilano R, Marichal T, et al. Neutrophil myeloperoxidase diminishes the toxic effects and mortality induced by lipopolysaccharide. *J Exp Med*. 2017;214(5):1249-58.
56. Stackowicz J, Jönsson F, Reber LL. Mouse Models and Tools for the in vivo Study of Neutrophils. *Front Immunol*. 2019;10:3130.
57. Zilionis R, Engblom C, Pfirschke C, Savova V, Zemmour D, Saatcioglu HD, et al. Single-Cell Transcriptomics of Human and Mouse Lung Cancers Reveals Conserved Myeloid Populations across Individuals and Species. *Immunity*. 2019;50(5):1317-34.e10.

6. Annex

6.1. Table of figures

- Figure 1.1 Detrimental effects and protective functions of neutrophils in myocardial infarction
- Figure 1.2 Neutrophil heterogeneity in myocardial infarction—polarization from N1 pro-inflammatory towards anti-inflammatory N2 over time
- Figure 1.3 Preliminary data from scRNAseq and CITE-seq analysis of cardiac neutrophils 1, 3 and 5 days after myocardial infarction
- Figure 1.4 Expression of SiglecF in isolated neutrophils at different time points
- Figure 3.1 Chart of ROS production activity assay
- Figure 3.2 Chart of phagocytosis activity assay
- Figure 4.1 Gating strategy of cardiac neutrophils
- Figure 4.2 Proportion and total number of cardiac neutrophils in the different cohorts.
- Figure 4.3 Side scatter (SSC)-A / Forward scatter (FSC)-A properties of Ly6G-SiglecF+ eosinophils, Ly6G+SiglecF low and Ly6G+SiglecF high neutrophils
- Figure 4.4 Proportion of SiglecFhigh neutrophils among total cardiac neutrophils
- Figure 4.5 Proportion of SiglecFhigh neutrophils among total bone marrow neutrophils
- Figure 4.6 Proportion of SiglecFhigh neutrophils among total blood neutrophils
- Figure 4.7 Proportion of SiglecFhigh neutrophils among total spleen neutrophils
- Figure 4.8 Proportion and total number of cardiac neutrophils in the different cohorts
- Figure 4.9 Proportion of SiglecFhigh neutrophils among total cardiac neutrophils
- Figure 4.10 Proportion of SiglecFhigh neutrophils among total blood neutrophils
- Figure 4.11 Immunofluorescence localization of SiglecF+ cells.
- Figure 4.12 Gating strategy of neutrophils incubated with PHrodo™ Green E. coli BioParticles® Conjugate
- Figure 4.13 Phagocytosis of E. coli bioparticles in neutrophil subsets
- Figure 4.14 Gating strategy of neutrophils incubated with DHR123
- Figure 4.15 Reactive oxygen species (ROS) production in neutrophil subsets
- Figure 4.16 Schematic chart of depleting and FACS antibodies binding themselves to the epitope 1A8
- Figure 4.17 Gating strategy of cardiac neutrophils gated as CXCR2+ cells

- Figure 4.18 Neutrophils can be reliably identified independently of surface Ly6G expression
- Figure 4.19 Experimental design of depletion experiment
- Figure 4.20 Anti-Ly6G treatment fails to achieve successful depletion of cardiac neutrophils 3 days after myocardial infarction
- Figure 4.21 Shift of SiglecF high neutrophils in the cardiac tissue of depleted mice
- Figure 4.22 Anti-Ly6G treatment fails to achieve complete depletion of blood neutrophils 3 days after myocardial infarction
- Figure 4.23 Anti-Ly6G treatment fails to achieve complete depletion of bone marrow neutrophils 3 days after myocardial infarction
- Figure 4.24 Anti-Ly6G treatment fails to achieve complete depletion of spleen neutrophils 3 days after myocardial infarction
- Figure 4.25 Anti-Ly6G treatment fails to achieve complete depletion of neutrophils 1 day after myocardial infarction
- Figure 4.26 Validation depletion experiment
- Figure 5.1 Graphical abstract

6.2. List of abbreviations

DAMPS	damage associated molecular patterns
DHR	Dihydrorhodamine
ECM	extracellular matrix
i.p.	intraperitoneal
IL	interleukin
LAD	left anterior descending coronary artery
MerTK	myeloid epithelial reproductive tyrosine kinase
MI	myocardial infarction
MMP	matrix metalloprotease
MPO	myeloperoxidase
NET	neutrophil extracellular traps
NGAL	neutrophil gelatinase associated lipocalin
ROS	reactive oxygen species
scRNAseq	single-cell RNA sequencing
TGF- β	tumor-growth-factor-beta
VEGF	vascular epithelial growth factor

6.3. Publication list

Vafadarnejad E*, Rizzo G*, **Krampert L***, Arampatzi P, Arias-Loza AP, Nazzal Y, Rizakou A, Knochenhauer T, Bandi SR, Nugroho VA, Schulz DJJ, Roesch M, Alayrac P, Vilar J, Silvestre JS, Zerneck A, Saliba AE, Cochain C. Dynamics of Cardiac Neutrophil Diversity in Murine Myocardial Infarction. *Circ Res.* 2020 Oct 9;127(9):e232-e249. doi: 10.1161/CIRCRESAHA.120.317200. Epub 2020 Aug 19. PMID: 32811295.

*Shared first authorship

6.4. Acknowledgements

Mein erster und großer Dank gilt allen Voran meinem Betreuer Clément und unserer Arbeitsgruppe. Mit viel Geduld, Hilfe, einem immer offenen Ohr und einer offenen Tür habe ich in dieser Zeit sehr viel gelernt und Spaß gehabt. Vielen Dank auch vor allem an Giuseppe, Dirk, Vallery, Anna und Sourish, mit euch zusammen ist man wirklich eine ArbeitsGRUPPE die sich hilft und unterstützt, und auch lange Tage im Labor haben viel Spaß gehabt.

Ein ganz großer Dank gilt meinen Eltern, die mir nicht nur bei sämtlichen bisherigen Entscheidungen meinen Freiraum gelassen und mich unterstützt haben, nun beruflich dort zu stehen wo ich bin, sondern mich auch über das gesamte Studium und darüber hinaus begleitet haben.

Und ein Dank von Herzen gilt meinem Mann Manuel, der immer motiviert, berät, bespaßt und unterstützt.

Vielen Dank!

6.5. Curriculum vitae

